Fatigue testing of carbide-free bainitic steels (Ensayo de fatiga de aceros bainíticos libres de carburos)

Alba M Díaz Rey

Tutor: Esa Vuorinen
Cotutora: María Jesús Lamela Rey

Universidad de Oviedo
Luleå University of Technology

RESUMEN EN ESPAÑOL

INTRODUCCIÓN

Se ha demostrado que la resistencia a la fatiga de los aceros bainíticos sin carburo es alta en comparación con los aceros templados. El shot-peening es un método que mejora la resistencia a la fatiga. En un proyecto anterior, acero con un tratamiento de shot-peening con alta intensidad se ensayó midiendo la resistencia a la fatiga. El objetivo de este proyecto es investigar la influencia del shot-peening con una menor intensidad sobre la resistencia a la fatiga de la estructura bainítica libre de carburo.

CONTEXTO

Los aceros bainíticos libres de carburo presentan una combinación de alta resistencia con buena ductilidad a bajo coste. La microestructura de estos aceros consta de bainita con ferrita y austenita retenida. Esto se puede lograr mediante un templado a una cierta temperatura seguido de un tratamiento isotérmico. La resistencia de estos aceros se debe a la pequeña escala de la microestructura, como las líneas de bainita, y las altas densidades de dislocación. La ductilidad se debe a la austenita retenida entre las líneas bainíticas. El efecto perjudicial de los carburos se equilibra reprimiendo la precipitación añadiendo una cierta cantidad de silicio.

Las probetas utilizadas en este ensayo han sido sometidas a un tratamiento de templado y posteriormente a un austempering. El tratamiento de temple consiste en la austenización del acero seguida de un enfriamiento lo suficientemente repentino como para obtener una estructura martensítica. Ya que el templado requiere de un tratamiento térmico posterior; el austempering es otro proceso de tratamiento común que evita la creación de distorsiones y grietas debidas a la refrigeración, lo que evita la necesidad de tratamientos adicionales para eliminar estos defectos. Este proceso comienza después de la cementación, el componente es templado hasta que alcanza una temperatura intermedia, más alta que la temperatura del Ms (entre 260-300 ° C). Durante un período de tiempo específico, la temperatura se mantiene constante, lo que permite la formación de bainita a partir de la austenita.

El shot-peening es un proceso diseñado para mejorar la resistencia a la fatiga de los componentes expuestos a altas tensiones alternas. Este tratamiento transforma las tensiones residuales de tracción en esfuerzos residuales de compresión, estos hacen que los componentes duren más. Este proceso se realiza en frío creando una capa de tensión residual de compresión que modifica las propiedades mecánicas del metal tratado. La superficie del componente es bombardeada con pequeñas bolas esféricas de acero, acero inoxidable, vidrio o cerámica de entre 0,1 y 3 mm de diámetro. Cada bola deja un hoyuelo creando deformación plástica local y debajo de la superficie, el metal intenta volver a su volumen inicial, lo que crea unas fuertes tensiones residuales de compresión. Estas tensiones están directamente relacionadas con el límite elástico del material. A medida que la superficie es bombardeada con miles de disparos, el componente queda envuelto en una capa sometida a tensión de compresión. Esta capa ayuda a prevenir las grietas por fatiga y mejora la resistencia al desgaste del componente.

El fallo por fatiga ocurre debido a la aplicación de tensiones fluctuantes que son menores que la tensión requerida para causar fallos durante una sola aplicación de ésta. La fatiga contribuye a aproximadamente un 90% de los fallos de servicio mecánico y es un problema que afecta a cualquier componente que se mueva. Se necesitan tres factores básicos para causar fatiga. Estos factores son: un esfuerzo de tracción máximo de valor suficientemente alto, una fluctuación suficientemente grande en el esfuerzo aplicado y un número suficientemente alto de ciclos del esfuerzo aplicado. También la vida de fatiga es la cantidad de ciclos que un componente puede soportar con un esfuerzo específico aplicado y el límite de fatiga es la tensión en la que por debajo de ésta el fallo no ocurre. La cantidad de ciclos que puede soportar una muestra es mayor cuando la tensión aplicada es menor. Los resultados de una prueba de fatiga pueden ser dispares, es importante probar un gran número de muestras para tener un valor estadístico preciso de los resultados.

Se han hecho estudios comparativos de probetas lisas y probetas con el tratamiento de shot-peening a fatiga. Después de las pruebas de fatiga de alto número de ciclos realizadas en flexión pura, se afirmó que el shot-peening aumentaba la vida de fatiga de los componentes al retrasar la iniciación y ralentizar la propagación de grietas. La relación entre el tiempo de iniciación y el tiempo de propagación es mayor en componentes con el tratamiento. En las probetas simples, la curva de crecimiento de la grieta muestra el retraso inicial y la aceleración posterior. Este retraso se debe a las barreras microestructurales que limitan la plasticidad de la punta de la grieta hasta que la concentración de la tensión en la barrera alcanza un valor crítico y la tasa de crecimiento de la grieta aumenta. Este estudio indica que cuanto mayor es la intensidad del shot-peening, mayor es la vida de fatiga. También que la relación del tiempo de iniciación sobre el tiempo de propagación aumentaba a medida que la intensidad aumentaba también.

En 2002, se realizó un estudio que analizaba la influencia del shot-peening en las pruebas de fatiga. Se hizo una comparación con probetas templadas frente a probetas con shot-peening a diferentes intensidades. Para estudiar cómo la intensidad influyó en la resistencia a la fatiga, las intensidades probadas fueron de 10, 15, 20, 25 y 30 A. Se encontró que el shot-peening mejoraba la vida de fatiga un 30%. Las intensidades óptimas se establecieron entre 20 y 25 A, se encontraron valores superiores a los que disminuyen la resistencia a la fatiga debido a la formación de grietas en la superficie y la reducción de la capa de tensiones residuales de compresión.

Otros estudios se llevaron a cabo en 2014 en los que se realizó un segundo shot-peening de baja intensidad después de un shot-peening de alta intensidad. El tratamiento de baja intensidad se realizó a 8 A o 5 A y la alta intensidad a 21 A. Este segundo tratamiento produjo un pequeño cambio en la superficie aumentando las tensiones residuales de compresión y se cree que restaura ligeramente la superficie dañada creada durante el tratamiento de alta intensidad pero no puede repararla por completo. Sin embargo, la influencia del shot-peening de baja intensidad no fue alta.

La cobertura del shot-peening es un factor importante para garantizar la calidad del tratamiento. Si la cobertura es inferior al 100% pueden desarrollarse grietas y disminuir la vida de fatiga del componente.

ENSAYO A FATIGA

Las probetas cilíndricas utilizadas en este ensayo a fatiga tienen una composición de 0.55C-1.72Si-0.74Mn-0.22Cr-0.18Ni-0.03Mo, con la siguiente geometría:

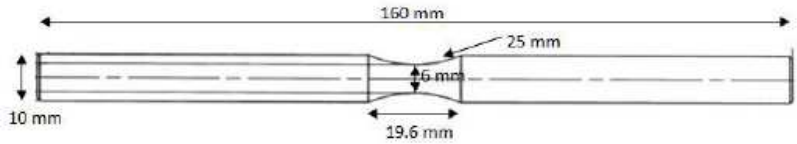

Figura 1. Dimensiones de las probetas

Las probetas se sometieron a un tratamiento térmico en dos pasos. Fueron austenizadas en un horno durante 30 minutos a 860 ° C. El segundo tratamiento fue un austempering en un baño de sal durante 60 minutos a 300 °C. Después de estos tratamientos se realizó un shot-peening en la curvatura central con disparos esféricos de hierro fundido con una intensidad Almen de 0,1 mmA. El ensayo a fatiga realizado fue una prueba de flexión rotativa realizada con una máquina modelo fabricada basada en una disposición de flexión de tres puntos. Esta máquina consistía en un motor, dos cojinetes de apoyo cerca y una celda de carga unida a un resorte. La carga se aplicó y aseguró con dos tornillos. La prueba se realizó a una frecuencia de 50 Hz y una velocidad constante de 3000 rpm y una relación de tensión R igual a -1. El valor de salida elegido fue $2.5 \cdot 10^6$ ciclos. La tensión elegida para comenzar esta prueba fue de 550 MPa. Siguiendo un método de escalera, los intervalos de tensión tomados fueron de 50 MPa, si la muestra se rompía entre los pasos la tensión se incrementó o disminuyó en 25 MPa. Después se calculó el límite de resistencia y la desviación estándar.

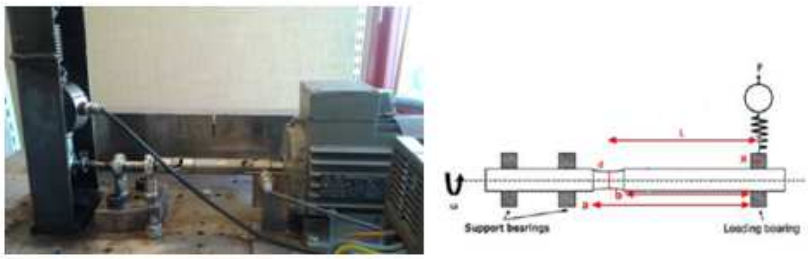

Figura 2. Configuración del ensayo a flexión rotativa.

Límite de fatiga:

$$R_{Fat\,(50\%)} = y_0 + d\left(\frac{A}{N-R} + \frac{1}{2}\right)$$

Desviación estándar:

$$s = 1.62 \cdot d\left(\frac{(N-R)\cdot B - A^2}{(N-R)^2} + 0.029\right)$$

$$A = \sum j(n_j - r_j)$$

$$B = \sum j^2 (n_j - r_j)$$

ANÁLISIS DE LA MICROESTRUCTURA Y DUREZA

Para estudiar la influencia de la intensidad del shot-peening en el acero con composición: 0.55C-1.72Si-0.74Mn-0.22Cr-0.18Ni-0.03Mo, se preparó una muestra de la sección transversal de un espécimen en el que se habían tratado sus dos superficies con diferentes intensidades (0,4 mmA y 0,1 mmA). Se cortó a un tamaño adecuado, se montó, y se pulió hasta 1 µm. Para estudiar la muestra en el microscopio óptico, se grabó con una solución de Nital al 3% durante 5 segundos. Para estudiarlo en SEM, se pulió durante 30 segundos en suspensión de sílice coloidal y se grabó de nuevo durante 4 segundos.

Para hacer un análisis del estudio de fractura, se realizó una muestra de la sección transversal de una probeta de fatiga rota. Se cortó, se montó y se pulió hasta 0,25. Para el microscopio óptico, se grabó con Nital al 3% durante 8 segundos. Para el SEM se volvió a pulir durante 30 segundos con suspensión de sílice coloidal y luego se grabó durante 4 segundos más. Esta muestra se desmontó de la baquelita con el fin de estudiar la superficie tratada con shot-peening en SEM.

Se tomó una muestra de la superficie de fractura de cada probeta fallida en la prueba de fatiga. Se estudiaron en SEM y después de un baño de ultrasonidos se analizaron en rayos X. Se tomó una muestra de referencia de una de las probetas testadas a fatiga para analizarla en también en rayos X. Se cortó y se pulió hasta 0,25 µm.

Las muestras mencionadas anteriormente se analizaron para estudiar la microestructura y la causa de la fractura. Estos análisis se realizaron en un microscopio óptico de luz Nikon y con un JEOL JCM-6000 SEM (microscopio electrónico de barrido).

Una prueba de difracción de rayos X se realizó con el fin de analizar el contenido de austenita retenida en el centro de las muestras rotas. Se analizaron tres muestras de las cinco probetas rotas junto con la referencia para lograr buenos resultados estadísticos. La prueba se realizó en un difractómetro PANalytical Empyrean. Los parámetros elegidos en el análisis fueron los siguientes: Un paso de tiempo de 700 segundos y un rango de ángulo de 40 a 70 grados. Las muestras se colocaron en un soporte y se introdujeron automáticamente una después de la otra para su análisis.

Se midieron varias muestras con una prueba de medida de la dureza Vickers en una máquina de microdureza MXT. Usando una carga de 50 kgf, se midió la dureza de ambas superficies tratadas a diferente intensidad. Después para la muestra de la sección transversal, se realizó un perfil midiendo la dureza de una superficie a otra con intervalos de 0,5 mm. Se hizo otro perfil de la dureza en la muestra de la sección transversal también con intervalos de 0,5 mm para ver cómo la dureza cambiaba más cerca de la superficie de la fractura.

La rugosidad de las dos superficies tratadas se midió con un perfilador óptico Veeco Wyko NT1100. El software proporciona una imagen en 3D de las superficies junto con los cálculos de los parámetros de rugosidad, como Ra (raíz media cuadrada), Rv (profundidad máxima del valle) y Rp (altura máxima del pico).

RESULTADOS EN LA INFLUENCIA DE LA INTENSIDAD DE SHOT-PEENING

Partiendo de las muestras del material para comparar intensidades se dieron los siguientes resultados:

La rugosidad es mayor para la superficie que se ha disparado con una intensidad más alta. En esta superficie hay huecos más profundos debido a la mayor velocidad del disparo y la mayor energía en el impacto que causó deformaciones plásticas profundas. En la superficie de menor intensidad hay más picos y huecos pero con una profundidad menor, que puede ser causada por un mayor número de disparos pero con menos energía en el impacto.

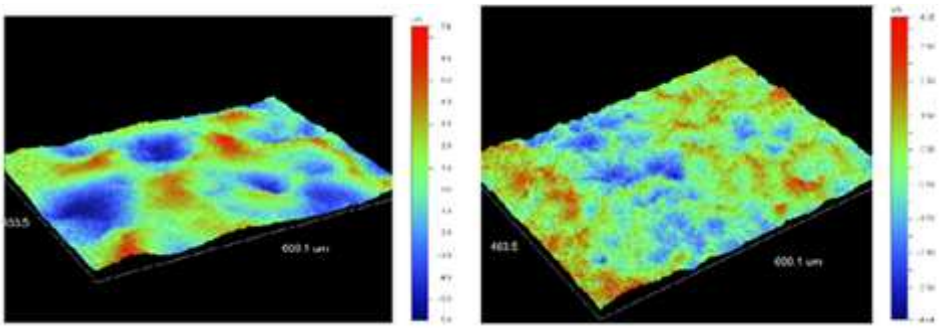

Figura 3. Rugosidad en las dos superficies

Después del estudio con el microscopio electrónico de barrido, las colonias de bainita se pueden observar con ferrita y austenita retenida. En ambas superficies no se puede apreciar ninguna transformación de fase inducida por shot-peening. Comparando ambas superficies no hay mucho cambio en la microestructura, aunque la superficie de más intensidad tiene una capa más profunda de disparos que la otra debido al cambio en la intensidad. Al comparar el material base, el tamaño del grano es más pequeño cerca de las superficies y más grande en el centro de la sección transversal. Esta reducción del tamaño de grano aumenta las propiedades mecánicas del componente tales como la resistencia y la dureza que son favorables para aumentar la resistencia a fatiga.

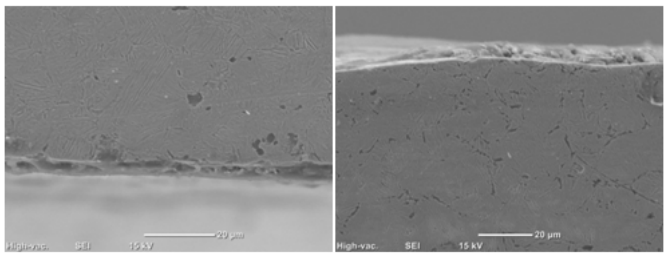

Figura 4. Resultados del microscopio electrónico de barrido

En cuanto a la dureza, se pudo observar que la superficie con más intensidad tenía una dureza mayor (673 HV) que la superficie de menor intensidad (660 HV). También se observó una

mayor dureza en la sección cercana a la superficie tratada en comparación con el centro de la muestra.

RESULTADOS DE LA INFLUENCIA DEL SHOT-PEENING EN FATIGA

En cuanto al ensayo de fatiga, los resultados fueron peores de lo que se esperaba aunque resultaron mejores en comparación con los estudios de shot-peening a una mayor intensidad. La mitad de las probetas sobrevivieron al ensayo y la otra mitad resultó en fallo. El límite a fatiga se estableció en 655 MPa cuando se esperaba un resultado de 990 MPa y la desviación estándar 86 MPa.

Probeta	Tensión (Mpa)	Ciclos	Fuerza (N)	Probetas sin fallo	Probetas rotas
1	550	2,50E+06	267	x	
2	650	2,50E+06	313	x	
3	750	427728	392		x
4	700	2500000	316	x	
5	800	167081	357		x
6	750	355329	365		x
7	700	2500000	301	x	
8	725	652834	351		x
9	700	123899	312		x
10	675	2500000	289	x	

En la muestra de la sección transversal de la probeta rota observada en el microscopio se puede ver en la microestructura, las líneas de ferrita rodeadas por finas películas de austenita retenida. Las colonias bainíticas tienen una orientación definida, fácil de ver. Se cree que los puntos negros son sulfuros de manganeso (MnS), pero después de un análisis los resultados no fueron claros, sin embargo, un alto contenido de carbono hace posible que sean inclusiones de grafito, que pueden aparecer si el contenido de carbono es superior al 20% para el material Fe-C, estos son defectos que están presentes en toda la superficie de la muestra y pueden provocar el inicio y la propagación de grietas que pueden causar fallos en el ensayo de fatiga.

En el análisis de las secciones de fractura de las probetas, los sitios de iniciación de las grietas se pueden encontrar siguiendo las líneas de propagación que emergen de la superficie. No se pueden encontrar grietas de iniciación claras, pero hay algunos defectos o huecos cerca de la superficie de iniciación que pueden causar el comienzo de la fractura. En una probeta, una inclusión fue la causa del fallo. En las probetas no fue común encontrar múltiples sitios de inicio de grietas. Es claro ver el sitio de iniciación en la superficie externa junto con los hoyuelos creados en el proceso de shot-peening.

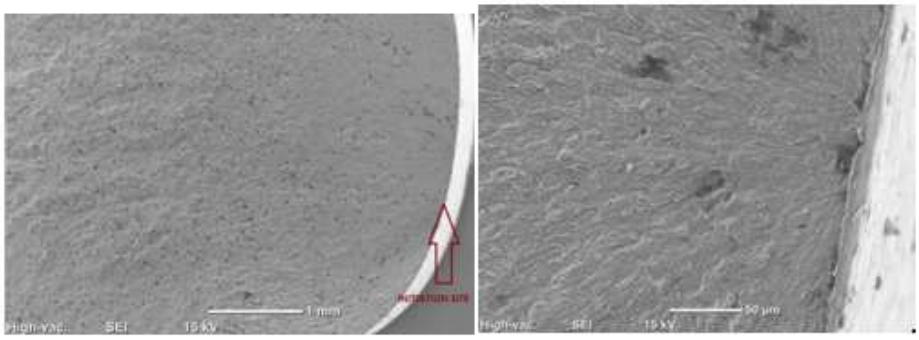

Figura 5. Iniciación de las grietas

Se realizó una prueba de difracción de rayos X para estudiar el contenido de austenita retenida en la superficie de fractura de tres muestras rotas y una muestra de referencia de una parte no rota de la probeta. Como se esperaba, el contenido de austenita retenida en la muestra de referencia es significativamente mayor en comparación con el contenido en las muestras rotas. Este hecho se debe a la transformación de la austenita en martensita causada durante la deformación en la fatiga. A medida que aumenta la tensión aplicada, el contenido de austenita retenida debería ser menor porque las deformaciones causadas son mayores. Sin embargo, en base a los resultados, esto no sucede en este estudio, el contenido de austenita retenida es mayor a medida que aumenta la tensión aplicada.

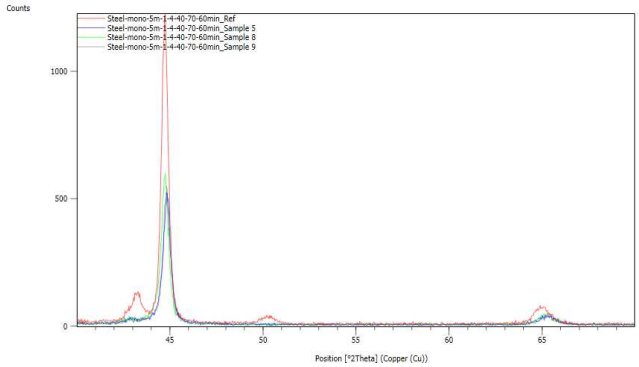

Figura 6. Resultados de la prueba de rayos X

Se midió la dureza de la sección transversal de una probeta rota. A partir del material de base, se tomaron varias medidas cada 0.5 mm con una carga de 50 kgf para observar el cambio en la dureza a medida que se acerca a la superficie de la fractura. La dureza disminuye más cerca de la superficie de fractura debido a la deformación causada en la prueba de fatiga con su fallo posterior.

De un trabajo anterior, se realizó un estudio de las tensiones residuales presentes en probetas con shot-peening con una intensidad de 0.4 mmA. Como se esperaba, las tensiones de compresión son más altas a medida que aumenta la profundidad, hasta que la profundidad no se ve influenciada por la superficie tratada y las tensiones tienden a cero.

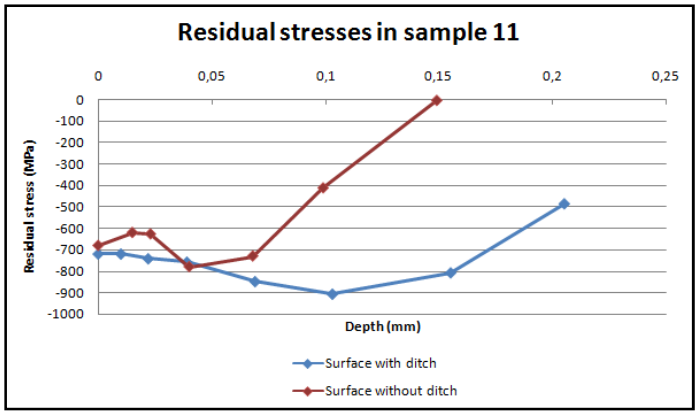

Figura 7. Tensiones residuales en una de las probetas

CONCLUSIONES

Después del estudio de las dos superficies tratadas con shot-peening a diferentes intensidades, las principales diferencias encontradas fueron:

El parámetro cuadrático medio de la rugosidad Ra fue mayor en la superficie con mayor intensidad, esta superficie tiene huecos más profundos debido a la mayor energía y al mayor tamaño de los disparos. Por otro lado, la superficie de menor intensidad tiene más huecos pero con menos profundidad debido a una menor energía y una mayor cantidad de disparos. En cuanto a la microestructura, no hay mucha diferencia entre las dos superficies, pero se puede observar que la capa de shot-peening es más profunda en la superficie de mayor intensidad. El tamaño de grano es más pequeño cerca de las superficies, lo que aumenta las propiedades mecánicas como la resistencia y dureza y mejora la fatiga vida del componente y resistencia a la fisuración por fatiga. Se confirmó que una mayor intensidad aumenta la dureza en la superficie y en aproximadamente 2 mm por debajo de la superficie.

Los resultados de las pruebas de fatiga no fueron tan exitosos como se esperaba. Se confirmó que una intensidad inferior a 0,4 mmA aumenta la vida de fatiga. Aunque las muestras que fallaron alcanzaron un número bajo de ciclos, el límite de resistencia fue mayor con una intensidad más baja que llegó a 655 MPa.

En el análisis de fractura se observó en la microestructura colonias de bainita con líneas de ferrita rodeadas por películas de austenita retenida. Las inclusiones de grafito se encontraron en toda la superficie creando defectos que podrían causar el inicio y la propagación de grietas. En la superficie de la fractura se encontraron sitios de iniciación de grietas. La inclusión fue la causa del fallo en una probeta. En la sección transversal de la superficie de la fractura, se encontraron los mismos defectos y huecos causados por la deformación continua de la fatiga. Éstos conducen y proporcionan una manera más fácil para que las grietas se expandan. Está claro que la grieta ocurre en las colonias bainíticas y se propaga a través de las películas de austenita. En la prueba de difracción de rayos X resultó un contenido más bajo de austenita retenida en la superficie de la fractura. Este hecho se debe al efecto que tiene lugar en las pruebas de fatiga en las que la austenita se transforma en martensita durante la deformación. Además, los resultados concluyeron que el contenido de austenita retenida es mayor a medida

que aumenta el estrés aplicado, que era lo contrario de lo esperado. Como se esperaba, la dureza disminuye más cerca de la superficie de la fractura.

En la prueba de fatiga, el límite de resistencia fue menor de lo esperado, sin embargo, se observó un aumento en la vida de fatiga en comparación con las probetas con shot-peening de mayor intensidad de estudios previos. El límite de resistencia fue de 655 MPa con una desviación estándar de 86 MPa. Se observó una transformación de la austenita retenida en martensita en la superficie de la fractura en los resultados de la difracción de rayos X debido al efecto causado durante la fatiga.

Se observó que la superficie con una intensidad mayor tenía una capa dañada más grande que puede causar un agrietamiento prematuro en la superficie durante las pruebas de fatiga. Se cree que las inclusiones de grafito que se encontraron mejoraron la propagación e iniciación de las grietas. Una muestra falló debido a la inclusión. Se observó que la iniciación de grietas se colocaba en la superficie.

Se han realizado estudios de probetas con un tratamiento de shot-peening a una intensidad de 0.4 mmA y 0.1 mmA. Para futuros trabajos, sería útil estudiar los parámetros del shot-peening para cambiarlos y mejorar el tratamiento superficial, reduciendo el daño a la superficie que es donde están los sitios de iniciación y manteniendo la capa de tensiones residuales de compresión.

También sería útil hacer un estudio más detallado de las inclusiones encontradas con grafito para estudiar su contenido de carbono y cómo esto afecta la iniciación y propagación de grietas en las pruebas de fatiga.

Sería útil realizar un estudio para comparar el centro de las probetas no tratadas y tratadas con el objetivo de estudiar cómo este tratamiento superficial afecta la transformación de la austenita en martensita durante la deformación en las pruebas de fatiga.

ACKNOWLEDGEMENTS

I would like to thank my supervisor Esa Vuorinen for guiding me through this project, for clarifying all my questions and for his dedication, effort and patience.

I am grateful for the technical support from the staff in the solid mechanics laboratory with the rotating-bending test machine.

I would also like to thank Johnny Grahn for his patience and for his help with all the equipment in the Material & science engineering department and Erik Nilsson for his assistance regarding the X-Ray diffraction test and its results.

ABSTRACT

Fatigue testing was made in samples of carbide-free bainitic steel of a composition 0.55C-1.72Si-0.74Mn-0.22Cr-0.18Ni-0.03Mo. The samples were previously austenitized at 860^{o}C and austempered in a salt bath at 300^{o}C. After these treatments the samples were shot peened with an Almen intensity of 0.1 mmA. The fatigue testing was made in a rotating-bending machine.

The results concluded that a lower intensity of shot peening helped achieve a better fatigue life. The endurance limit was established in 655 MPa which was less than the endurance limit expected. Crack initiation was found in the surface. It was stated that this fact was caused by the damaged surface from the shot peening and the presence of inclusions of graphite that favored the crack propagation reducing the fatigue life of the samples.

TABLE OF CONTENTS

1. INTRODUCTION

Fatigue resistance of carbide-free bainitic steels has been shown to be high in comparison with quenched and tempered state of the steel. Shot-peening is a method that improves the fatigue resistance. In previous project, shot-peening with high intensity has been tested by measuring the fatigue resistance. The aim of this project is to investigate the influence of shot-peening with a lower intensity on fatigue resistance of carbide-free bainitic structure.

2. BACKGROUND

2.1 Carbide-free bainitic steels

For an eutectic reaction, pearlite only takes place at a high temperature between 550 and 720^{o}C and the formation of martensite occurs at a low temperature. There is a range of temperatures in between (250-550 ^{o}C) in which none of these phases forms. In this range, fine aggregates of ferrite plates or laths and cementite particles are formed. The name of this intermediate structure is bainite. Bainite also occurs during athermal treatments at cooling rates too fast for pearlite to form but not rapid enough to produce martensite (Honeycombe & Bhadhesia, 1995,115). There are two forms of bainite known as upper and lower bainite. Both consist of aggregates of laths of ferrite, separated by regions of residual phases such as untransformed austenite or martensite or cementite. The reason why there is retained austenite adjacent to the bainitic ferrite is that its carbon concentration grows because of the transformation, the growth of bainite becomes thermodynamically impossible. If the starting carbon concentration of the steel is large, the formation of bainite stops at an earlier stage of the reaction and the amount of residual phases becomes larger.

The upper bainite forms at temperatures between 550 and 400°C. The microstructure of upper bainite consists of fine plates of ferrite that grow into clusters called sheaves. Within each sheaf the plates are parallel and have the same orientation. The individual plates in a sheaf are separated by low-misorientation boundaries or by cementite particles.

The lower bainite forms at temperatures between 400 and 250°C. The microstructure of the lower bainite is very similar to the upper, the most noticeable difference is that carbides also precipitate inside the plates of ferrite. There are two kinds of precipitates: those which grow from the carbon-enriched austenite which separates the platelets of bainitic ferrite, and others which appear to precipitate from supersaturated ferrite.

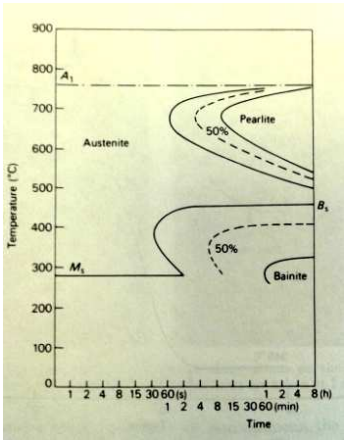

Figure 1. TTT curves for a Fe-3Cr-0.5C wt% steel. Honeycombe & Bhadhesia (1995)

As seen in figure 1, as the isothermal transformation temperature goes below B_s, lower bainite is obtained in which carbides precipitate in the ferrite with a reduced amount of precipitation from the austenite between the ferrite. The transition from upper to lower bainite is explained in terms of the rapid tempering processes that happen after the growth of a supersaturated plate of bainite.

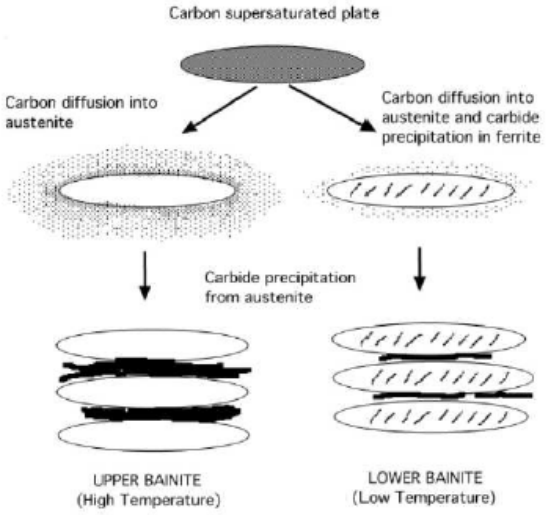

Figure 2. Schematic representation of the transition from upper to lower bainite. Honeycombe & Bhadhesia (1995)

Excess carbon partitions into the residual austenite by diffusion but the supersaturation can be reduced by precipitation of the carbides in the ferrite. At high temperatures the diffusion is fast and the precipitation of carbides in the ferrite is not possible, creating an upper bainitic microstructure. Cementite eventually precipitates from the carbon-enriched residual austenite.

When the transformation temperature decreases and the carbon diffusion is slower, some carbon precipitates as fine carbides in the ferrite. The rest partitions into the austenite, in order to precipitate as inter-plate carbides, creating a lower bainitic microstructure. The inter-plate carbides are smaller than the ones in the upper bainite because only a fraction of the carbon partitions into the austenite.

In this case, only lower bainite is obtained from steels containing higher concentrations of carbon and in low carbon steels only upper bainite is obtained.

Carbide-free bainitic steels present a combination of high strength with good ductility at a low cost. The microstructure of these steels consist of bainite with ferrite and retained austenite. This can be achieved by quenching to a certain temperature followed by an isothermal holding temperature treatment.

The strength of these steels is due to the small scale of the microstructure such as the bainite lathes, and the high dislocation densities. The ductility is due to the retained austenite between the bainitic lathes. The prejudicial effect of the carbides is balanced by repressing the precipitation adding a certain amount of silicon.

By adding silicon on the upper bainite reaction, the formation of cementite from austenite is retarded and so resulting in a bainitic ferrite and austenite microstructure.

Despite of that, the bainitic ferrite-austenite microstructure has some inconvenients. Sometimes blocky regions of austenite can be found between the sheaves of bainite, these regions have a tendency to transform into high carbon, untempered martensite under the influence of small stresses and then have an embrittling effect. Some films of austenite appear between the plates of ferrite, but these are more stable because of their higher carbon concentration and the constraint to transformation from the surrounding plates of ferrite.

Table 1. Chemical compositions (wt%) of experimental high strength steels with microstructures consisting of mixtures of bainitic ferrite and retained austenite. Bhadeshia (1992)

C	Si	Mn	Ni
0.22	2.0	3.0	-
0.4	2.0	-	4.0

Typical compositions of high strength steels that show good toughness as seen in table 1, sometimes have similar properties (sometimes these can be improved by tempering at slightly higher temperatures than the transformation temperature in which the bainite formed) than martensitic alloys that have been quenched and tempered . This comparison can be seen in Figure 3.

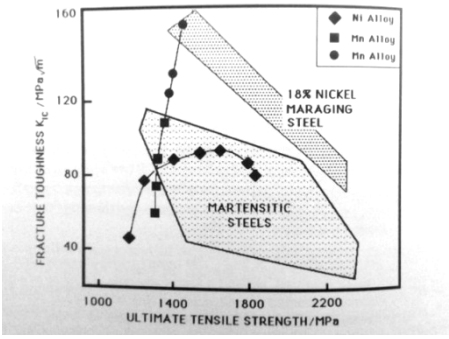

Figure 3. Comparison of the mechanical properties of mixed microstructures of bainitic ferrite and austenite, versus those of quenched and tempered martensitic alloys. Bhadeshia (1992)

2.2 Heat treatments

The modification of the structure and properties of a metal or alloy as a result of controlled heating and cooling is called a heat treatment. In steels there are different types of heat treatments, the ones that do not modify the chemical composition of the components and the ones that induce new chemical elements. Every heat treatment goes through three steps: heating, constant temperature and cooling.

The most common heat treatment in steels is quenching and tempering which allows an increase of the hardness. Quenching treatment consists in austenitization of the steel followed by cooling sufficiently sudden as to obtain a martensitic structure. The posibility of quenching a steel depends on two factors: the hardenability of the steel (TTT curves situation) and the cooling rate, which depends also in the cooling medium and the size of the work piece to be hardened. The quenching of steel is never a final treatment since the martensitic structure obtained, although it is very hard, at the same time is very fragile because of the strong generated internal stresses around the carbon atoms trapped in the iron cell. After quenching it is necessary to do a heat treatment of tempering that consists in heating the steel until it reaches a lower temperature with the purpose of obtaining a structure that although it has a lower hardness and resistance, will be tougher and more ductile.

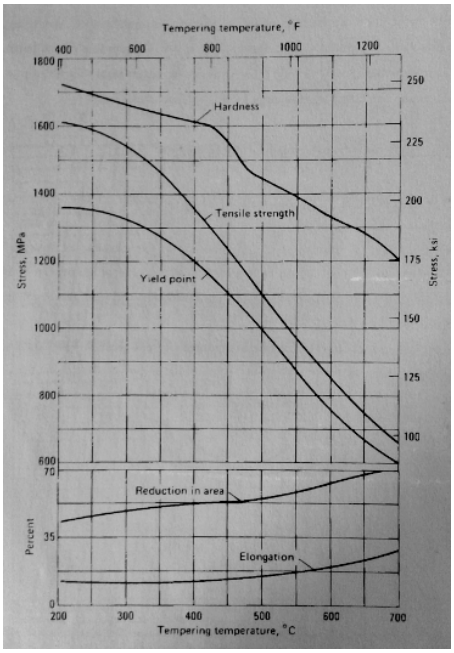

Figure 4. Evolution of the mechanical properties of the steel A130 (0.3C-0.5Mn-0.25Si-1Cr-0.2Mo) as a function of the tempering temperature.(Belzunce & Viña, 2011)

Austempering is another common treatment process that decreases the risk for creation of distortions and cracks from the cooling, this avoids the necessity of additional treatments to remove these defects. A higher toughness is obtained for a given hardness compared to the tempering. This process begins after austenitizing, the component is quenched until it reaches an intermediate temperature, higher than the M_s temperature (between 260-300^{o}C). For an specific amount of time the temperature is maintained constant allowing the formation of

bainite from austenite. This quenching is made by introducing the component in a salt bath. After that, the component is washed with water and air cooled. This treatment also reduces the chance of hydrogen embrittlement. This process is represented in figure 5.

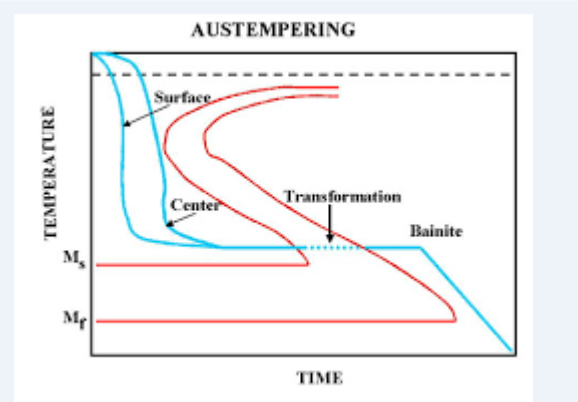

Figure 5. Austempering. (Belzunce & Viña, 2011)

2.3 Shot peening

Shot peening is a process designed to improve the fatigue resistance of components exposed to high alternating stress. Other surface treatments such as grinding, milling and bending along with other heat treatments can create tensile residual stresses which decreases the life of these components. Instead, shot-peening transforms the tensile residual stresses into compressive residual stresses, these make the components last longer.

This process is cold working creating a compressive residual stress layer changing the mechanical properties of the metal treated. The surface is bombarded with small spherical balls made of steel, stainless steel, glass or ceramic between 0.1 and 3 mm of diameter. Each ball leaves a dimple creating local plastic deformation and beneath the surface, the metal tries to return to its initial volume which creates strong compressive residual stress. This stress is directly related to the elastic limit of the material. As the surface is bombarded with thousands of shots, the component becomes encased in a compressively stressed layer. This layer helps prevent the fatigue cracks and stress corrosion and enhances the wear resistance of the component.

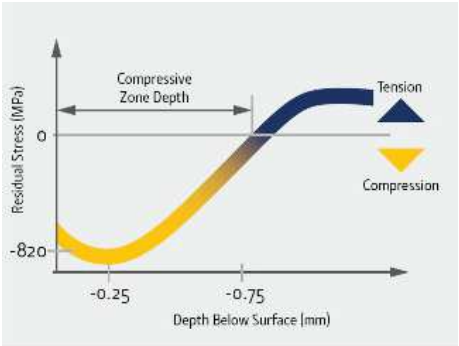

Figure 6. Residual stresses in shot-peening.(Wheelabrator shaping industry)

Full coverage of a shot-peened surface is essential in order to achieve a high quality. Coverage is the relations between the initial surface and the surface covered in dimples, it should never be less than a 100% because fatigue cracks and stress corrosion can develop in an area without impacts. Some materials can have better results with a coverage higher than 100%.

Shot peening intensity is the measure of the energy of the flow of the balls which is in direct relation with the compressive stress induced in a component. The intensity can be increased by using balls of a bigger size or by increasing their speed. Other variables that influence the intensity are the shot angle and the material of the balls. The intensity is controlled by measuring the energy being imparted by the shot. This is made by using an Almen strip fabricated to strict tolerances of hardness and flatness. This strip is shot peened on one side and the induced compressive stresses result in the bowing or curving of it. The curvature is proportional to the energy imparted by the shot. The strip arc height varies with the speed and size of the ball. The saturation of the component is considered to be achieved if while the exposure time is doubled, the arc height increases a 10% or less.

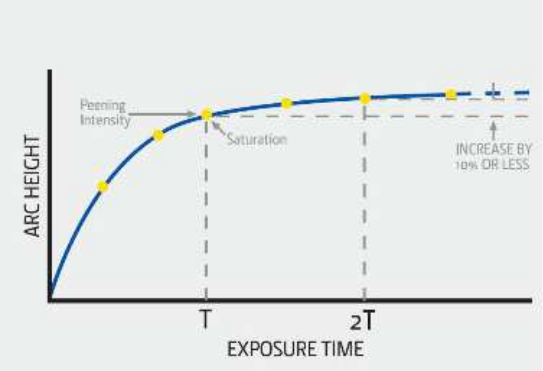

Figure 7. Control process. (Wheelabrator shaping industry)

2.4 Residual stresses

Residual stresses are locked-in stresses placed within a metal component. The residual stresses are present in the component without it being exposed to external forces or thermal gradients. Those stresses are generated by processes that constrain a part of the component from expanding or contracting, this is done as a response of the material to a non-uniform distribution of plastic strain. The manufacturing processes that cause these residual stresses are heat or mechanical treatments. There are two types of stresses: tensile and compressive.

Some factors that can cause tensile residual stresses are the development of deformation gradients in various sections of the component by the development of thermal gradients, volumetric changes created during the solidification or from solid state transformations. They can also appear in a component that is made from different materials because of the different coefficient of thermal expansion. Thermal residual stresses are due to the difference in the expansion when a metal is heated or cooled. Also when a component is formed through cold working, residual stresses can appear.

The residual stresses can be large enough in a metal to cause distortion or cracking. The presence of surface tensile stresses can contribute to stress corrosion and fatigue cracking. It is an important factor to control the magnitude of these tensile residual stresses in order to avoid these facts that can cause the failure of the component. The magnitude of these stresses can be controlled by the adjustment of heat treatment processes, by selecting alloys that provide slower cooling rates.

On the other hand the compressive residual stresses are not as harmful as the tensile stresses. They can help to prevent the fatigue cracks and stress corrosion and enhance the wear resistance. This stresses are beneficial and allow the component to endure. Compressive residual stresses are usually intentionally induced through some manufacturing processes like shot peening, as mentioned before in 2.3. In figures 6 and 8 the distribution of residual stresses in a shot peened surface can be observed.

Figure 8. Stresses in a shot peened surface. (Wheelabrator shaping industry)

.

2.5 Fatigue

Fatigue failure occurs due to the application of fluctuating stresses which are lower than the stress required to cause failure during a single application of stress. Fatigue contributes to approximately a 90% of mechanical service failures and is a problem that affects any component that moves (Campbell, 2008).

Three basic factors are needed to cause fatigue. These factors are: a maximum tensile stress of sufficiently high value, a large enough fluctuation in the applied stress and a sufficiently large number of cycles of the applied stress. There are various types of fluctuating stresses as seen in Figure 9. Also the fatigue life is the number of cycles that a component can endure with an specific stress applied and the endurance limit is the stress below which failure does not occurs. The number of cycles that a specimen can endure is higher when the applied stress is lower. The results of a fatigue test can be scattered, it is important to test a high number of specimens in order to have an accurate statistic value of the results.

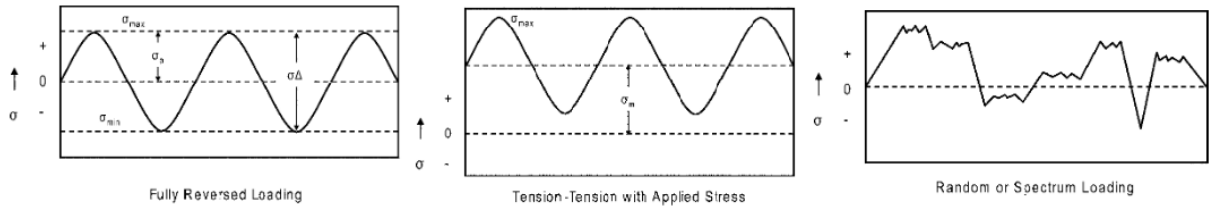

Figure 9. Different types of fluctuating stresses. (Campbell, 2008)

There are two kinds of tests regarding the number of cycles, high-cycle and low-cycle fatigue. High-cycle fatigue takes place in tests with a number of cycles higher than 10^5 and an applied stress low enough to be elastic. It is also used with high-strength steels. Endurance limit of high-strength steels is very sensitive to surface condition, residual-stress state, and presence of inclusions. This favors small crack formation which propagate slowly in a direction perpendicular to the tensile axis. The cross-section area is reduced to the point that it cannot endure the load and the specimen fails. The material response is macroscopically elastic, the crack growth period is relatively short compared with the crack initiation period (Campbell, 2008).

In low-cycle fatigue, macroscopic plastic deformation occurs in every cycle and failure can occur in a small number of cycles (1000 or less cycles). A high stress level is applied, because of this final failure will occur when the cracks are small, periods of visible crack growth are not present (Schijve,2001). During cyclic loading within the elastic regime, stress and strain are related by the elastic modulus. For cyclic loading that produces plastic strains, the responses form a hysteresis loop. As seen in Figure 10. The component is in tension from point O to point A. The unloading of the strength is represented by the curve A to D. In D the specimen is not under stress. The component is in compressive stress from D to B. Reapplying tensile stress the component returns to A (Campbell, 2008).

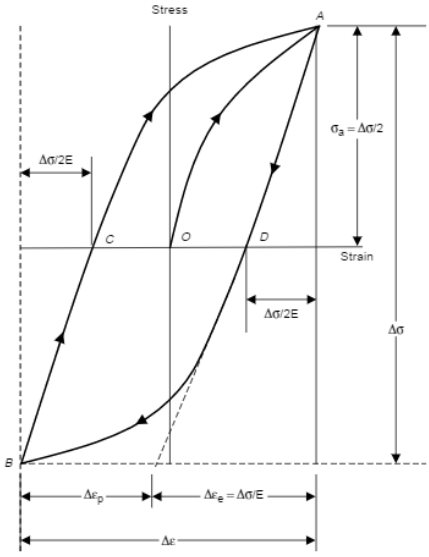

Figure 10. Stress-strain hysteresis loop for cyclic loading. (Campbell, 2008)

The total strain (Δε) consists of both elastic and plastic components as seen in equation 1.

$$\Delta\varepsilon = \Delta\varepsilon_e + \Delta\varepsilon_p \qquad (1)$$

The fatigue life of a component can be improved by inducing residual compressive stresses on the surface. This can be achieved by shot peening as mentioned before and by surface rolling with contoured rollers. Two processes that can also improve the fatigue life by inducing compressive residual stresses are the carburization and nitriding usually used to improve wear resistance. Other surface-hardening methods such as flame or induction hardening produce similar effects.

Regarding the crack propagation in carbide-free bainitic steels not many studies have been made.

Fatigue crack growth process is divided in three regions; region I of slow expanding crack propagation, region II of stable expansion and region III of rapid expansion.

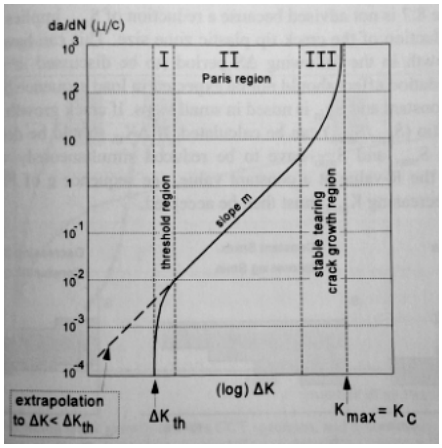

Figure 11. Three regions of the crack growth rate. (Schijve,2001)

A study made by Rementeria (2015) with samples that went through early cracking with initiation of cracks at the surface states that in region I the crack grows along the active slip bands immediately after the initiation. Grain and phase boundaries act as barriers against slip transmission into adjacent grains so this reduces the shear displacement at the crack tip and decelerates the propagation. Due to this fact grain refinement increases the fatigue strength of the material.

TRIP-effect (Transformation induced plasticity) occurs when retained austenite transforms into martensite during plastic transformation in fatigue as illustrated in figure 12. Due to the production of high carbon martensite the component becomes brittle, favoring the creation of cracks or the propagation. Initiation sites can also be caused by inclusions.

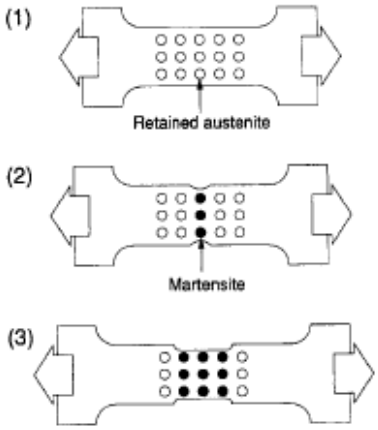

Figure 12. Illustration of TRIP-effect. (Yokoi ,1996)

A study made by Wenyan (1997) states that at low stress intensity factor ΔK levels (threshold region), the fatigue crack grows at a low speed along phase boundaries or through filmy austenite contained by two or three grains. This fact is due to the low ΔK levels in that region so the fatigue crack cannot grow across the bainite lathes that are stronger. The crack grows along the slip plane of the retained austenite. In the plastic deformation region, the high deformation strengthening ability of the austenite improves the resistance to slip, this makes it more difficult for the fatigue crack to grow. This was also studied by Yokoi (1995) as shown in Figure 13, the relation between the number of cycles and the volume fraction of retained austenite in tests performed with an applied stress of 470 MPa.

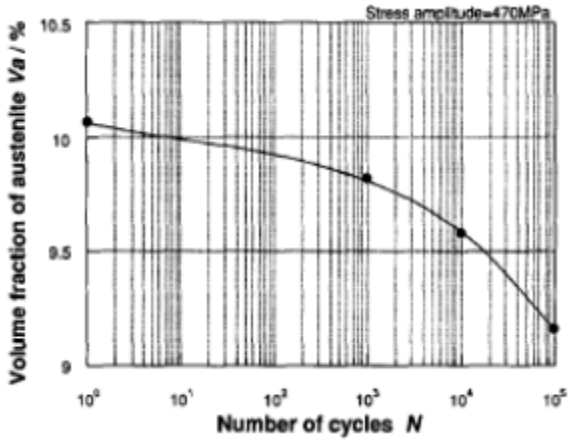

Figure 13. Relation between the number of cycles and the volume fraction of retained austenite Va/% . (Yokoi, 1995)

2.6 Shot peening effect in fatigue

As mentioned before, shot peening induces in the components a compressive stressed layer that helps prevent the fatigue cracks, stress corrosion and enhances the wear resistance.

In 1995 a study was made by De los Ríos in which the fatigue crack initiation and propagation of shot peened and unpeened samples were analyzed. After high-cycle fatigue test performed in pure bending it was stated that shot peening increased fatigue life of the components by delaying initiation and slowing propagation of cracks. The ratio of initiation time to propagation time is higher in shot peened components. The time in the early stages of crack growth is proportionally higher in the shot peened samples. As can be seen in Figure 14, shot peening affects the crack growth within the short crack region. In the plain specimens the crack growth curve shows the initial retardation and the posterior acceleration. This retardation is due to the microstructural barriers constraining crack tip plasticity until the stress concentration at the barrier reaches a critical value and the crack growth rate increases. This study states that the higher the intensity of shot peening, the higher the fatigue life. Also that the ratio of initiation time over propagation time increased as the intensity increased too.

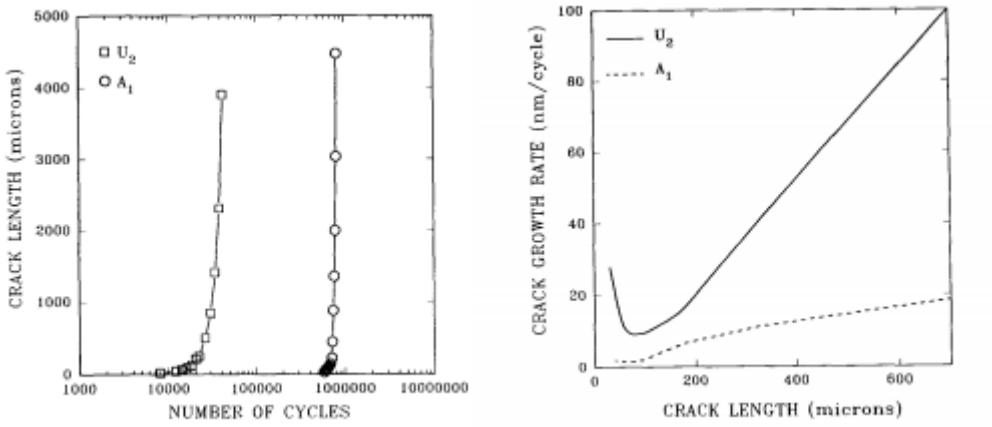

Figure 14. Crack growth of peened (A1) and unpeened (U2) specimens tested at equivalent stress and crack growth comparison of crack propagation (De los Rios, 1995).

In 2002 a study was made by Tekeli analyzing the influence of shot peening in fatigue testing. A comparison was made with quenched and tempered samples versus shot peened samples at different intensities. To study how intensity influenced the fatigue strength the intensities tested were 10, 15, 20, 25 and 30 A. Shot peening was found to improve the fatigue life a 30%. Optimum shot peening intensities were established between 20 and 25 A, values higher than those were found to decrease fatigue strength because of the formation of cracks at the surface and reduction of the compressive residual stress layer.

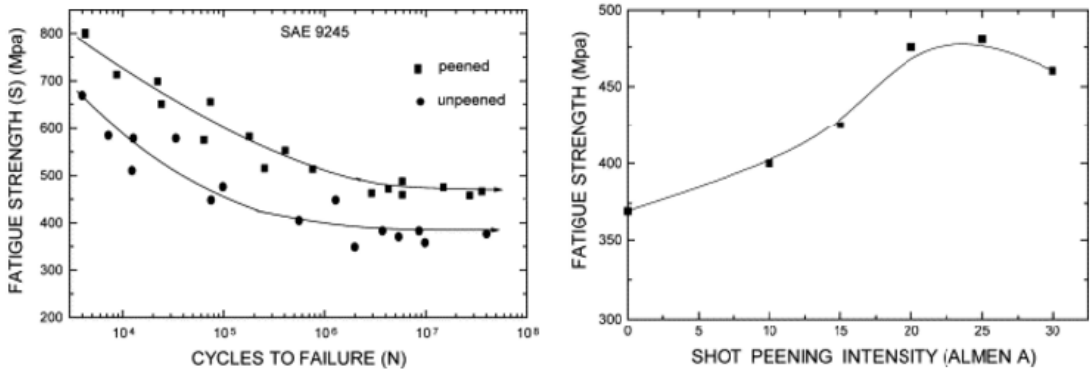

Figure 15. S-N curves and effect of shot peening intensity on fatigue strength.

Studies were made by Vielma in 2014 in which a second low intensity shot peening was performed after a high intensity shot peening. The low intensity treatment was performed at 8 A or 5 A and the high intensity at 21 A. This second treatment produced a small change in the surface increasing compressive residual stresses and it is believed to slightly restore the damaged surface created during the high intensity treatment but it is not able to completely mend it. However, the influence of the low intensity shot peening was not high.

As mentioned before, the coverage of the shot peening is an important factor to ensure the quality of the treatment. If the coverage is less than 100% fatigue cracks can develop and decrease the fatigue life of the component.

3. FATIGUE TESTING

The samples studied in this study apart from the shot-peening intensity, all have the same characteristics than the ones studied in previous work performed by Kianzad (2015).

The composition of the samples is: 0.55C-1.72Si-0.74Mn-0.22Cr-0.18Ni-0.03Mo. The samples are cylindrical with a diameter of 10 mm, a length of 160 mm. In the center they were machined with a curvature of 25 mm of radius and a length of 19.6 mm, the diameter at the center is 6 mm. All the dimensions can be seen in Figure 16:

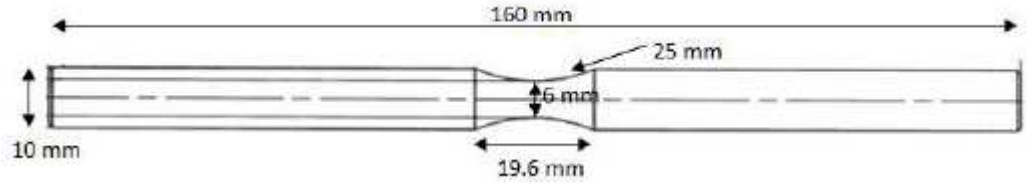

Figure 16. Dimensions of the sample. (Siamak, 2015)

The samples were put through a heat treatment in two steps. They were austenitized in an oven for 30 minutes at 860^{o}C. The second treatment was an austempering in a salt bath for 60 minutes at 300 ^{o}C.

After these treatments, the samples were shot-peened at the curvature in the center. The shot-peening was performed with spherical cast iron shots with an Almen intensity of 0.1 mmA, see Figure 17.

Figure 17. Shot peened sample.

The fatigue test performed was a rotating-bending test done with a manufactured model machine based on a three-point bending arrangement. This machine consisted in a motor, two support bearings close to it and a load cell attached to a spring. The load was applied and secured with two screws. The test was performed at a frequency of 50 Hz and a constant speed of 3000 rpm and a stress ratio R equal to -1. The run-out value chosen was $2.5 \cdot 10^{6}$ cycles.

Figure 18. Rotating bending test set up.

The force applied in the load cell was calculated with the following equations starting from the chosen stress applied at the center of the sample in each test.

Modulus of a circle:

$$W_b = \frac{\pi \cdot d^3}{32} \qquad (2)$$

Distance from the load bearing to the center:

$$L = \frac{a - b}{2} + b + x \qquad (3)$$

Stress applied at the center:

$$\sigma = \frac{M}{W_b} = \frac{F \cdot L}{\frac{\pi \cdot d^3}{32}} \qquad (4)$$

So clearing the equation the force applied is:

$$F = \frac{\pi \cdot d^3 \cdot \sigma}{32 \cdot L} \qquad (5)$$

The dimensions of the sample are cleared in Figure 19:

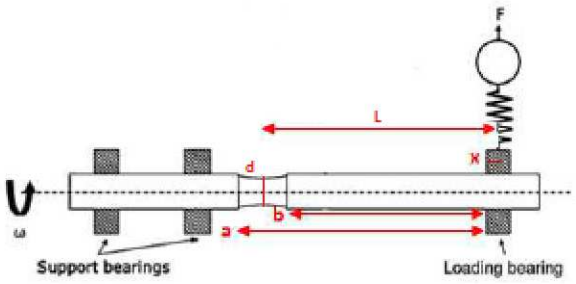

Figure 19. Scheme of the variables needed to calculate the applied force.

As in previous work by Kianzad (2015) the endurance limit obtained was between 500 and 560 MPa, the stress chosen to begin this tests was 550 MPa. Following a staircase method, the stress intervals taken were 50 MPa, if the sample broke between steps, the stress was increased or decreased 25 MPa.

After using this staircase method, the endurance limit and standard deviation is calculated. The model used in this project is the same as the one used by Kianzad (2015) in order to compare and because failure was as common as the success. The equations used to calculate the endurance limit and the standard deviation are the following:

Endurance limit:

$$R_{Fat\,(50\%)} = y_0 + d\left(\frac{A}{N-R} + \frac{1}{2}\right) \qquad (6)$$

Standard deviation:

$$s = 1.62 \cdot d\left(\frac{(N-R)\cdot B - A^2}{(N-R)^2} + 0.029\right) \qquad (7)$$

$$A = \sum j(n_j - r_j) \qquad (8)$$

$$B = \sum j^2(n_j - r_j) \qquad (9)$$

Where y_0 is the minimum stress level for a successful test, d is the stress interval, N is the total number of tests and R is the number of failed samples.

5. ANALYSE OF MICROSTRUCTURE AND HARDNESS

5.1 Sample preparation

To study the influence of the intensity of shot peening in the steel with composition: 0.55C-1.72Si-0.74Mn-0.22Cr-0.18Ni-0.03Mo, a sample of the cross section of a specimen in which two surfaces have been shot peened at different intensities (0.4 mmA and 0.1 mmA) was prepared. It was cut to a suitable size, mounted, grinded and polished down to 1 µm and after that a finishing step with colloidal silica suspension was applied. In order to study the sample in the optical microscope, it was etched with a solution of Nital 3% during 5 seconds. In order to study it in SEM, it was polished during 30 seconds in colloidal silica suspension and etched again during 4 seconds.

Figure 20. Surface 1 shot peened at 0.4 mmA, surface 2 shot peened at 0.1 mmA and sample of cross section.

One sample from each surface was polished with 1 µm to create flat islands in the rough surface in order to measure the hardness.

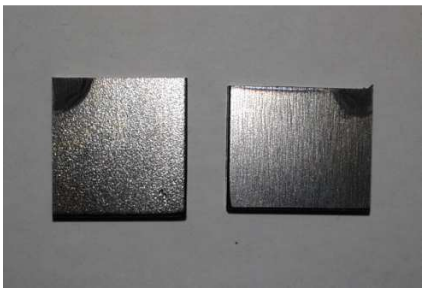

Figure 21. Hardness samples of surface 1 and 2 respectively.

To make an analysis of the fracture study, a sample of the transversal section from a broken fatigue sample was made. It was cut, mounted, grinded and polished down to 0.25 µm and polished as a final step with colloidal silica suspension. For the optical microscope it was etched with Nital 3% during 8 seconds. For the SEM it was polished again during 30 seconds with colloidal silica suspension and then etched during 4 more seconds. This sample was removed from the bakelite in order to study the shot peened surface in SEM.

Figure 22. Broken specimen and transversal section sample.

A sample of the fracture surface was taken from every failed sample in the fatigue testing. They were studied in SEM and after an ultrasonic bath they were analyzed in XRD. A reference sample was taken from one of the samples tested in fatigue in order to analyze it in XRD. It was cut, grinded and polished down to 0.25 µm and polished as a final step with colloidal silica suspension.

Figure 23. Sample of the fracture surface and reference sample.

5.2 Microstructure and fracture analysis

The samples mentioned before were analyzed in order to study the microstructure and the cause of the fracture. Those analysis were performed in a Nikon light optical microscope and with a JEOL JCM-6000 SEM (Scanning electron microscope).

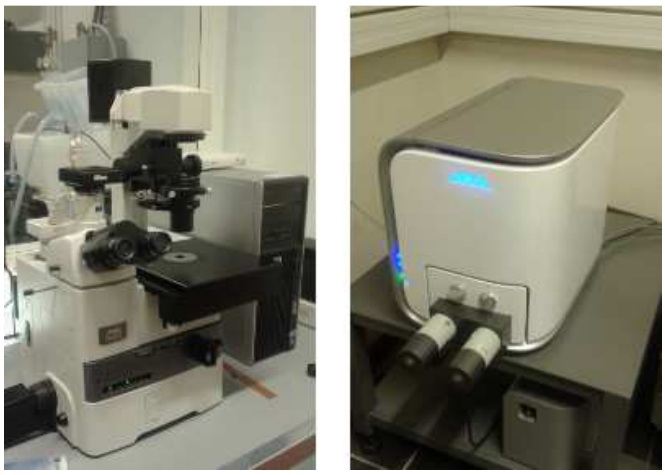

Figure 24. Nikon light optical microscope and JEOL JCM-6000 SEM.

5.3 XRD

The X-ray diffraction test was made in order to analyze the content of retained austenite in the center of the broken samples. Three samples of the five broken specimens were tested along with the reference in order to achieve good statistic results. The test was performed in a PANalytical Empyrean diffractometer. The parameters chosen in the analysis were the following: A time step of 700 seconds and an angle range from 40 to 70 degrees. The samples were positioned in a holder and introduced automatically one after the other for their analysis.

Figure 25. PANalytical empyrean diffractometer and sample placed in the holder.

5.4 Hardness

Several samples were measured with a Vickers hardness measure test in a MXT microhardness machine. Using a load of 50 g, the hardness of both surfaces 1 and 2 was measured. Then for the sample of the cross section, a profile was made by measuring the hardness from surface 1 to surface 2 with intervals of 0.5 mm. Another profile of the hardness was made in the transversal section sample also with intervals of 0.5 mm to see how the hardness changed closer to the fracture surface.

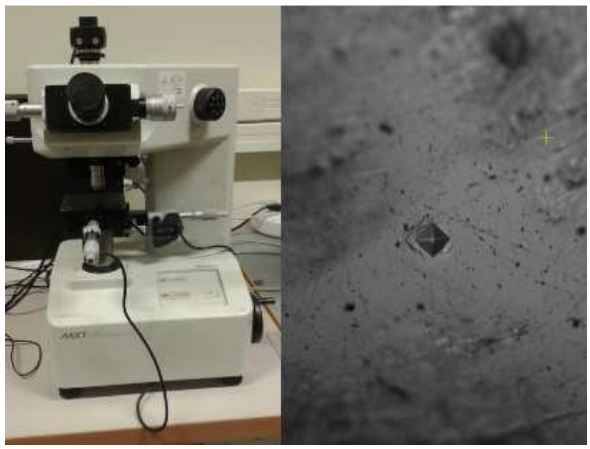

Figure 26. MXT microhardness machine and capture from a test.

5.5 Roughness

The roughness of surface 1 and surface 2 of the shot peened sample with different intensities in each side was measured with a Veeco Wyko NT1100 Optical profiler. The software gives a 3D image of the surfaces along with the calculations of the roughness parameters such as R_a (root mean square), R_v (maximum valley depth) and R_p (maximum peak height).

Figure 27. Veeco Wyko NT1100 Optical profiler.

6. RESULTS

6.1 Influence of shot-peening intensity

6.1.1 Roughness

The following are the results for the parameter R_a which is the average of the deviations from the mean value.

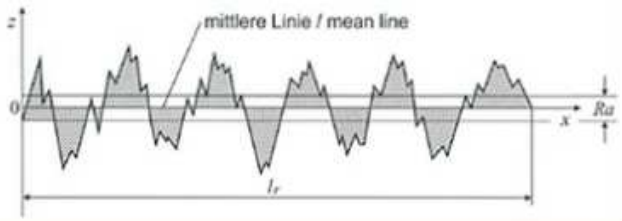

Figure 28. Ra: arithmetical mean deviation.

As can be seen in Table 2, the R_a is larger for the surface 1 which has been shot-peened with a higher intensity. In Figures 29 and 30 can be observed that in the surface 1 there are deeper hollows due to the higher velocity of the shot and the higher energy in the impact which caused deep plastic deformations. In surface 2 there are more peaks and hollows but with a lower depth, which can be caused by a larger number of shots but with less energy in the impact.

Table 2. Results of the Ra.

Surface	Intensity	Ra (μm)
1	0,4	1,797
2	0,1	0,951

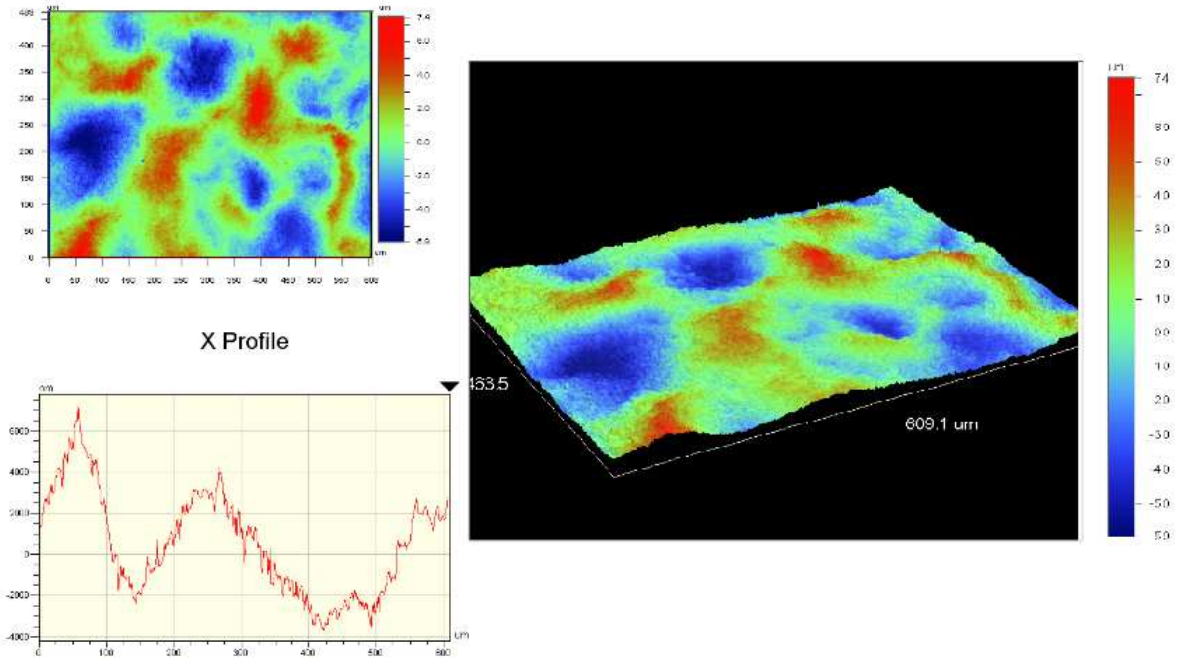

Figure 29. Profile and 3D image of the surface 1

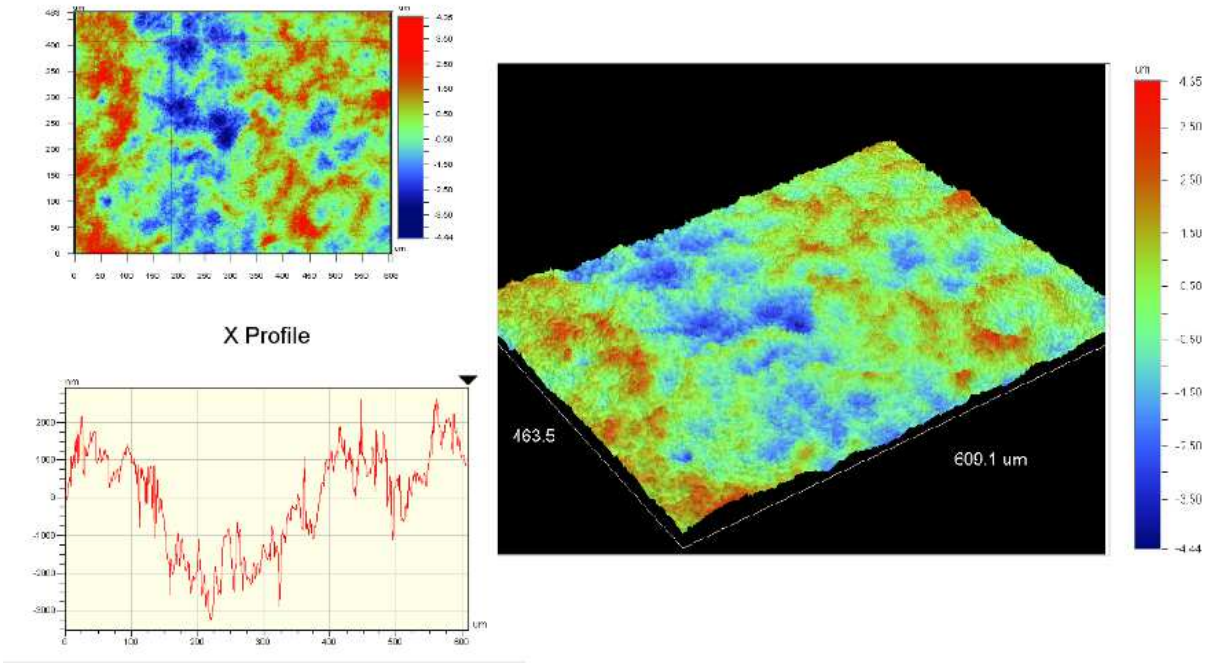

Figure 30. Profile and 3D image of the surface 2

6.1.2 Microstructure

The cross section was studied both in light optical microscope and in SEM with the following results:

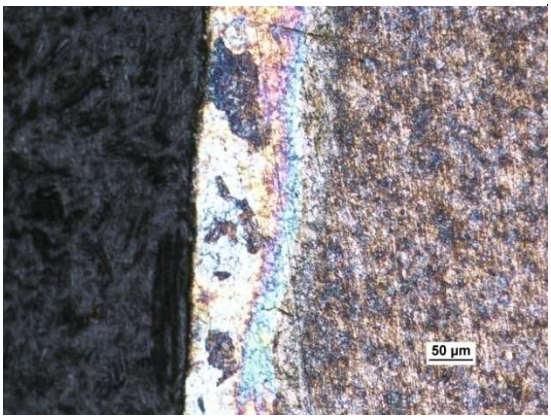

Figure 31. Surface 1 in OM with a magnification of x20

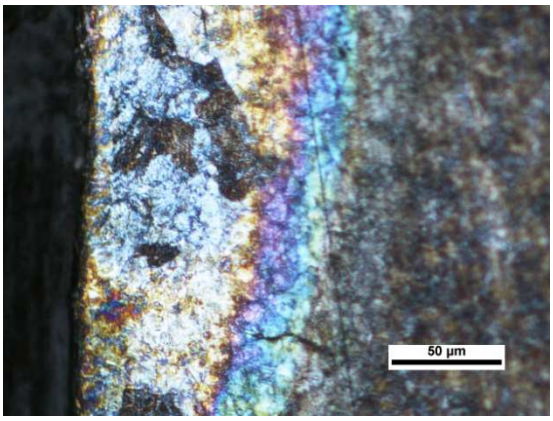

Figure 32. Surface 1 in OM with a magnification of x50

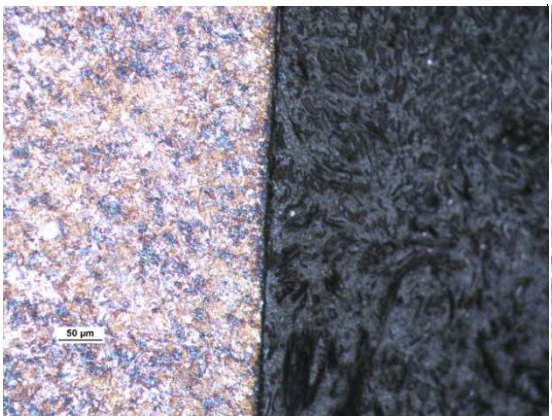

Figure 33. Surface 2 in OM with a magnification of x20

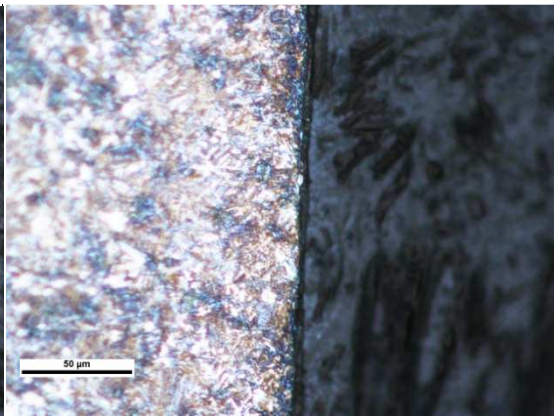

Figure 34. Surface 2 in OM with a magnification of x50

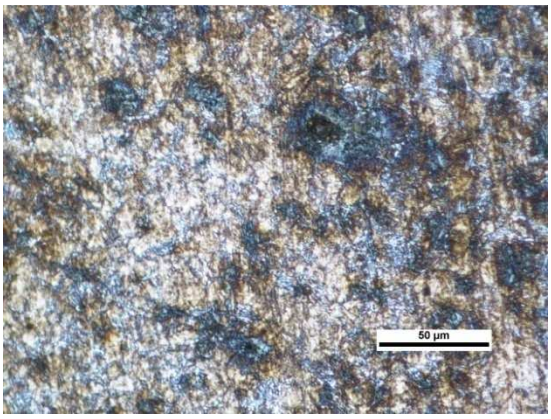

Figure 35. Bulk material in OM, magnification of x50

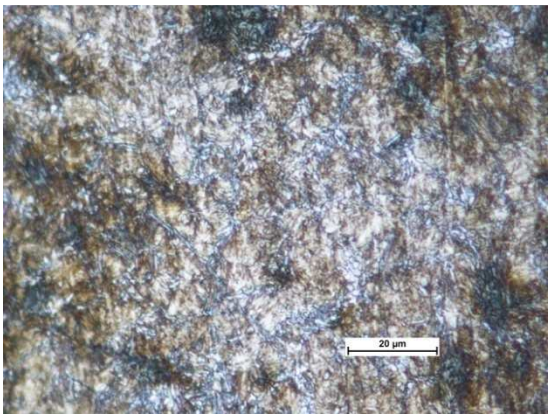

Figure 36. Bulk material in OM, magnification of x100

In the pictures the bainite colonies can be observed with ferrite and retained austenite. In both surfaces cannot be appreciated any phase transformation induced by shot peening. Comparing both surfaces there is not much change in the microstructure although the surface 1 has a deeper shot peened layer than the surface 2 due to the change in the intensity. Comparing the bulk material, the grain size is smaller near the surfaces and bigger at the center of the cross section. This grain size reduction increases the mechanical properties of the component such as strength and hardness which are favorable to increase the fatigue crack resistance.

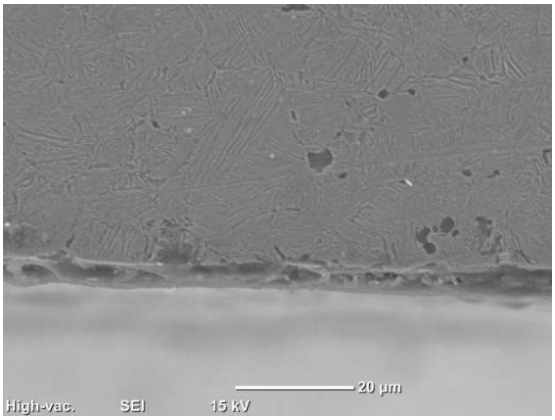

Figure 37. Surface 1 in SEM

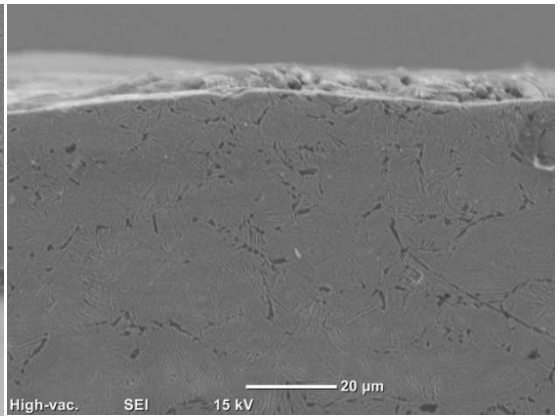

Figure 38. Surface 2 in SEM

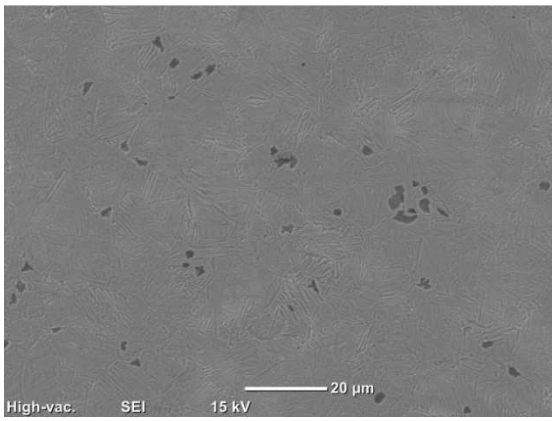

Figure 39. Bulk material in SEM

The same observations can be seen with the SEM pictures, the bainite colonies, the ferrite and the retained austenite are more clear along with the grain size reduction as it gets closer to the surfaces. In these pictures, the depth of the shot peened layer is more clear. It is larger in the surface 1 and more superficial in surface 2. Other pictures can be found in Appendix 1.

6.1.3 Hardness

The hardness in the samples of the both surfaces was measured on the top of the islands polished before. 15 measures were taken from each surface to achieve an accurate mean value of the hardness. In surface 1 the hardness was 673 HV, and surface 2 was 660 HV confirming that a higher intensity gives a higher hardness. Complete data with the 15 measures can be found in Appendix 2.

The hardness of the cross section was studied taking measures from surface 1 to surface 2 with an interval of 0.5 mm. In Figure 40 it can be observed that the hardness in surface 1 is higher, than in the bulk material where the hardness is constant and it increases close to surface 2 reaching a lower value than in surface 1.

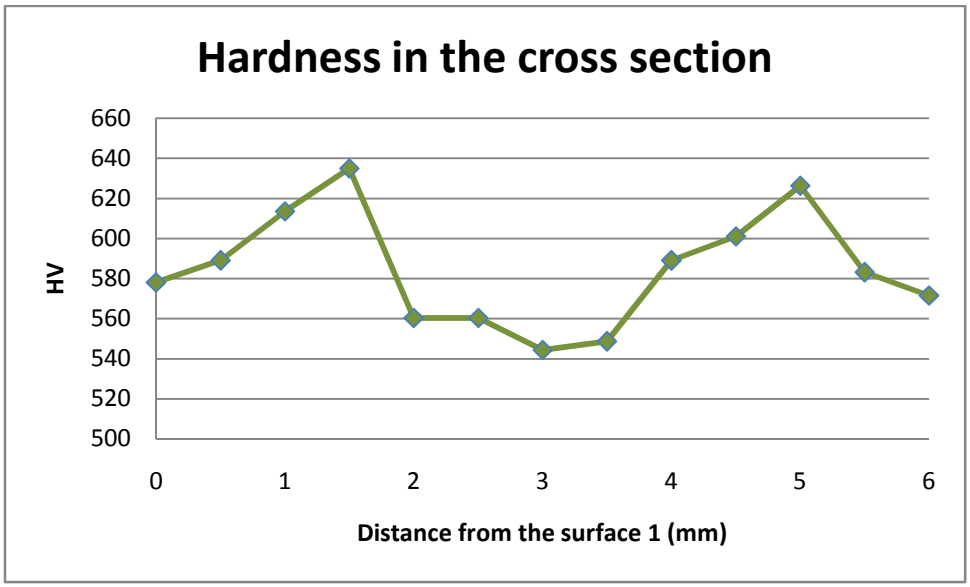

Figure 40. Hardness in the cross section.

6.2 Shot-peening in fatigue test

6.2.1 Fatigue test

The results obtained in this experiment were expected to be better than the tests done before by Kianzad (2015) with a higher shot-peening intensity. The results indeed were better, half of the samples survived and half of them failed. However the samples that failed reached a low number of cycles. They were expected to endure at a stress of 990 MPa based on the previous experiments performed by Leiro (2014). By observing the results in Table 3 and Figure 41 and after the calculations made from the equations 6-9, the endurance limit was established at 655 MPa and the standard deviation was 86 MPa.

Table 3. Data of fatigue test.

Sample	Stress (Mpa)	Cycles	Force (N)	Run-out	Failure
1	550	2,50E+06	267	x	
2	650	2,50E+06	313	x	
3	750	427728	392		x
4	700	2500000	316	x	
5	800	167081	357		x
6	750	355329	365		x
7	700	2500000	301	x	
8	725	652834	351		x
9	700	123899	312		x
10	675	2500000	289	x	

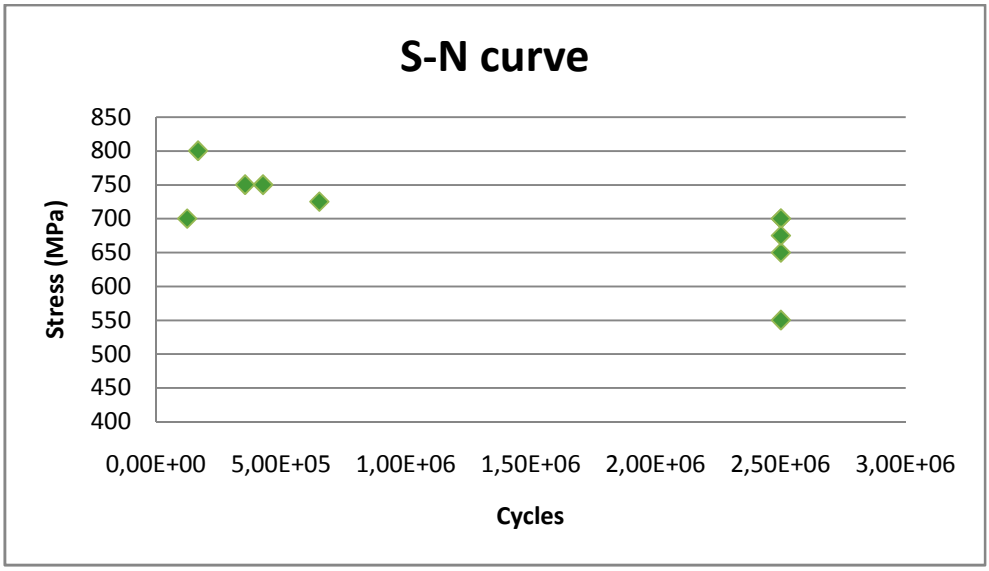

Figure 41. S-N curve for fatigue results.

6.2.2 Microstructure

A sample of the transversal section of the broken samples was analyzed in the optical microscope and in SEM in order to study the microstructure closer to the fracture surface.

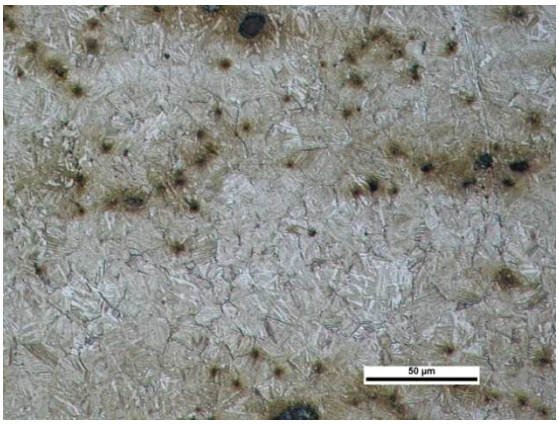

Figure 42. Transversal section in OM with a magnification x50

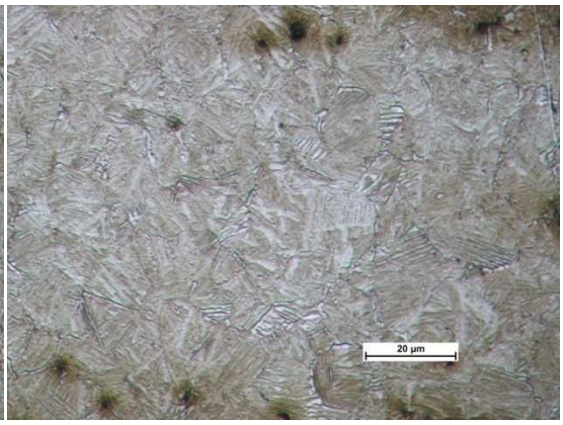

Figure 43. Transversal section in OM with a magnification x100

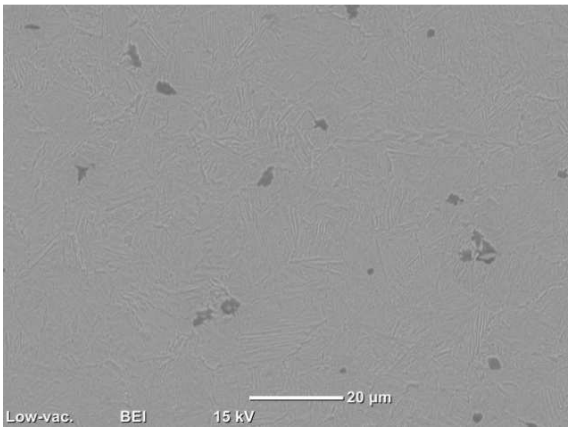

Figure 44. Transversal section in SEM

In the microstructure ferrite laths can be observed surrounded by fine films of retained austenite, blocky austenite was difficult to distinguish. Bainite colonies have a defined orientation easy to see. The black spots are believed to be manganese sulfides (MnS), but after an analyze the results were not clear, a high carbon content makes it possible for them to be graphite inclusions, that can occur if the carbon content is higher than 20 wt% for the Fe-C material but this is not a possible result in this case. These are defects that are present in all the surface of the sample can cause initiation and propagation of cracks that can cause failure in the fatigue test. The results of the analysis of the inclusions can be found in Appendix 5.

6.2.3 Fracture analysis

First the fracture surface of the broken samples was studied in SEM. Initiation sites can be found with propagation lines emerging from the surface. No clear initiation points can be found but in Figure 46 there are some defects or voids close to the initiation surface which can cause the beginning of the fracture. In a sample an inclusion was the cause of the failure as can be seen in Figure 47. In the samples was not common to find multiple crack initiation sites. Initiation of the fracture failure was common at the surface.

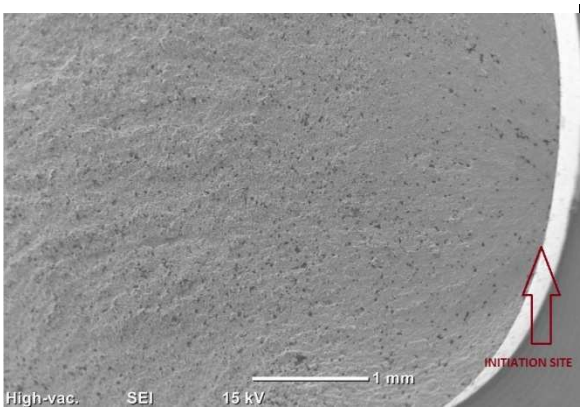

Figure 45. Initiation site.

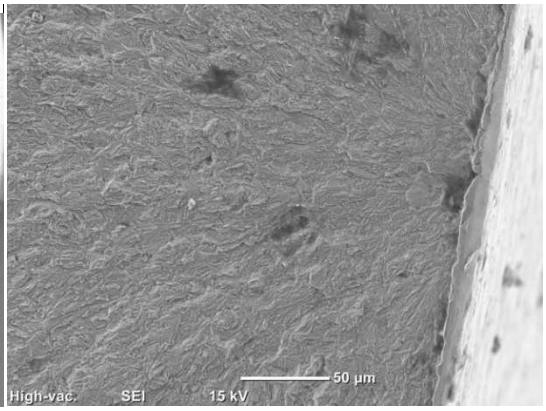

Figure 46 Closer capture of the initiation site.

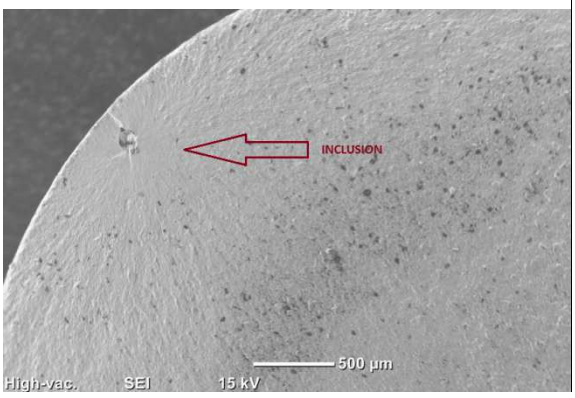

Figure 47. Inclusion

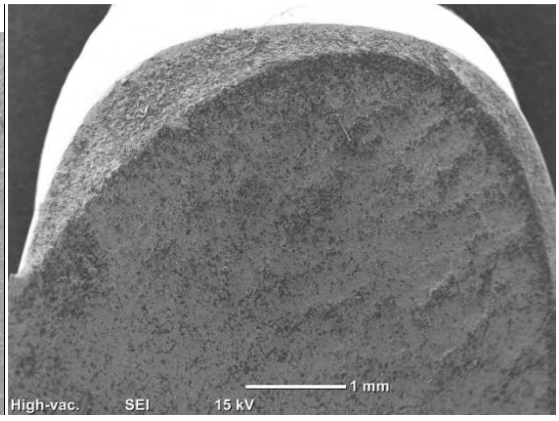

Figure 48. Fracture section.

After this, the transversal section of the fracture surface was studied both in light optical microscope and SEM. Inclusions can be found in all of the surface along with voids caused by the continuous deformation in the fatigue testing. These defects provide an easy way for the cracks to expand and cause failure. In Figure 50 these defects can be found close to the fracture surface. In Figures 51 and 52 taken in SEM, it can be seen that the initiation of the fracture is caused by a defect on the surface and lead to another defect in the centre of the sample. In Figure 53 a crack initiation site is clear and in Figure 54 can be observed that the crack occurs in the bainitic colonies and goes through the filmy retained austenite.

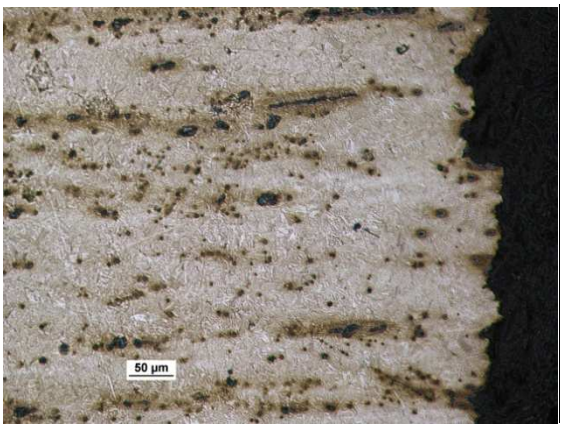

Figure 49. T-S in OM with a magnification of x20

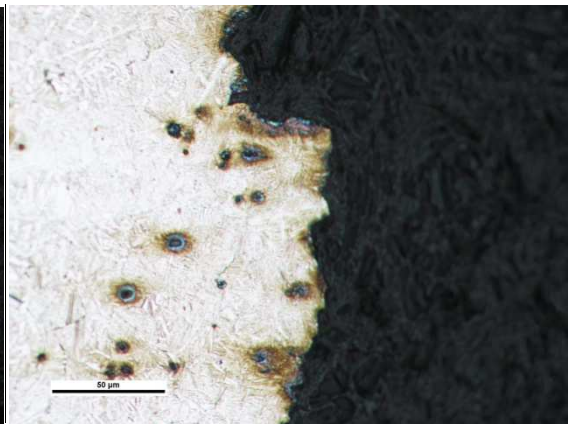

Figure 50. Defects close to the fracture surface. (x50)

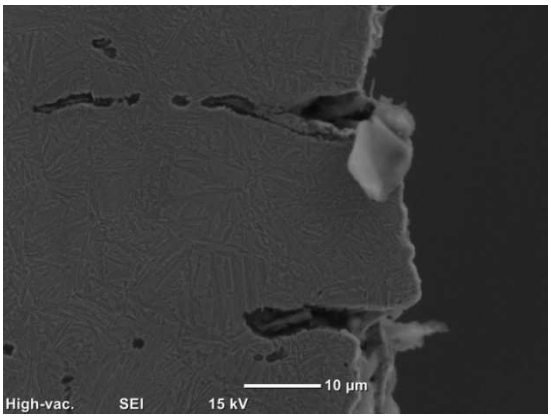

Figure 51.Voids in the transversal section.

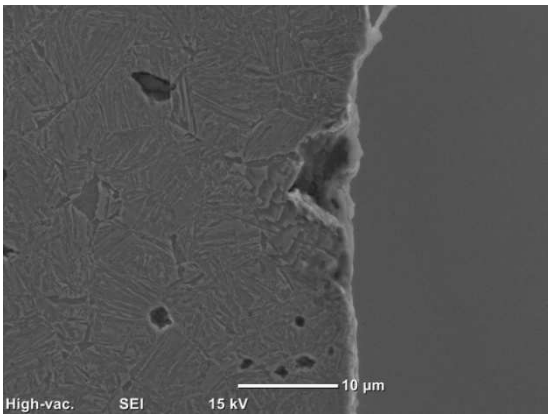

Figure 52. Defects in the transversal section.

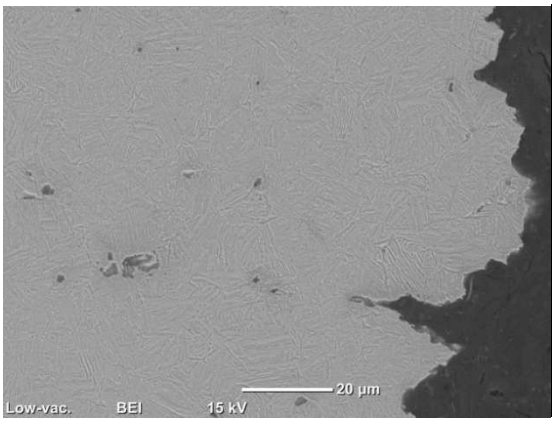

Figure 53. Crack initiation.

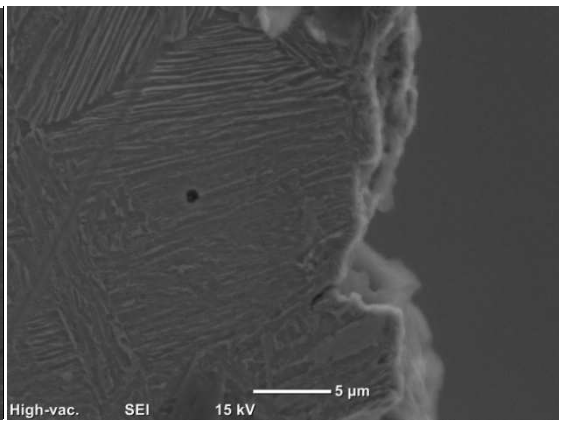

Figure 54. Fracture in austenite film.

The shot peened surface of the fracture was also analyzed in SEM. It is clear to see the initiation site in the outer surface along with the dimples created in the shot peening process. More pictures of the fracture analysis can be found in Appendix 3.

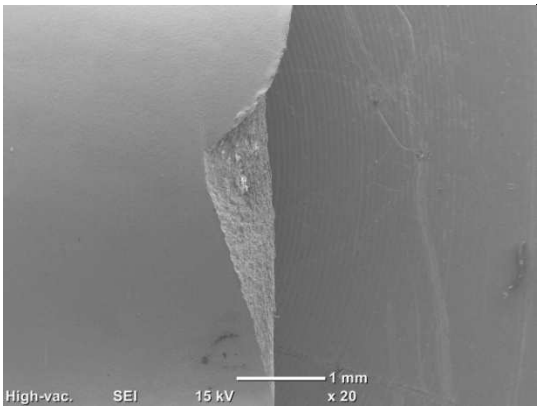

Figure 55. Initiation site.

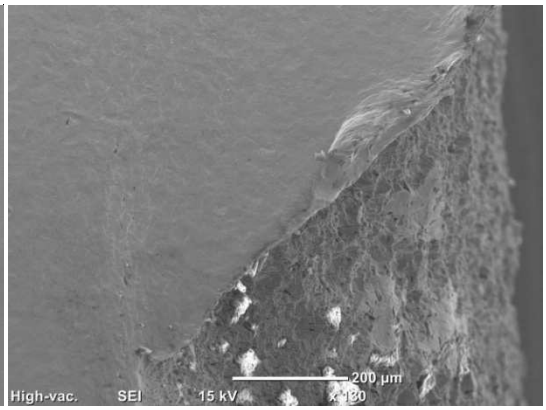

Figure 56. Initiation site.

6.2.4 XRD

X-ray diffraction test was made in order to study the content of retained austenite in the fracture surface of three broken samples and a reference sample from an unbroken part of the specimen. Four peaks were obtained in the results. Two main peaks can be seen in Figure 57, the first peak takes place at 43^{o} representing the content of austenite and a second peak at 45^{o} that represents the ferrite. There are two more peaks at 50^{o} and 65^{o} that represent austenite and ferrite. As expected, the content of retained austenite in the reference sample is significantly higher comparing with the content in the broken samples. This fact is due to the transformation of the austenite into martensite caused during deformation (TRIP-effect).

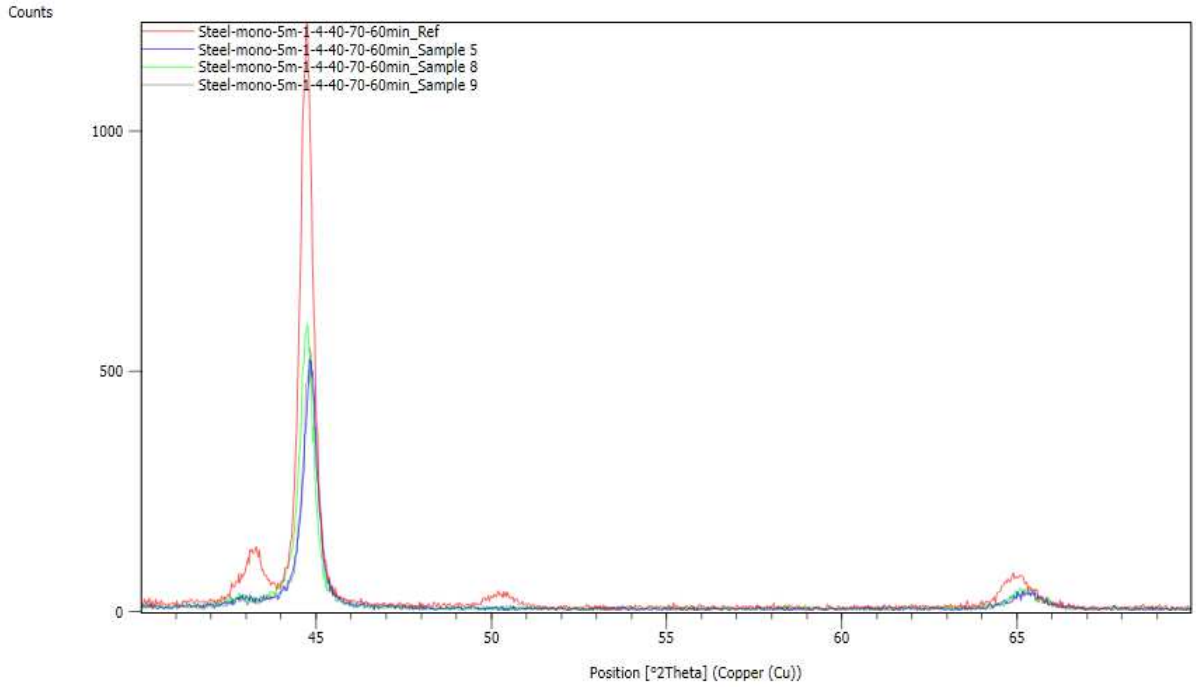

Figure 57. XRD results.

As the applied stress increases the content of retained austenite should be lower because the deformations caused are higher. However based on the results from Table 4, this does not happen in this study, the content of retained austenite is higher as the applied stress increases.

Table 4. Results of XRD.

Sample	Austenite content (wt%)	Ferrite content (wt%)	Stress (Mpa)
Reference	10,8	89,2	-
5	4,4	95,5	800
8	2,1	97,9	725
9	1,3	98,7	700

6.2.5 Hardness

Hardness of the transversal section of a broken sample was measured. Starting from the bulk material, several measurements were taken every 0.5 mm with a load of 50 g in order to observe the change in the hardness as it gets closer to the fracture surface. As can be seen in Figure 58 the hardness decreases closer to the fracture surface due to the deformation caused in the fatigue testing with its posterior failure.

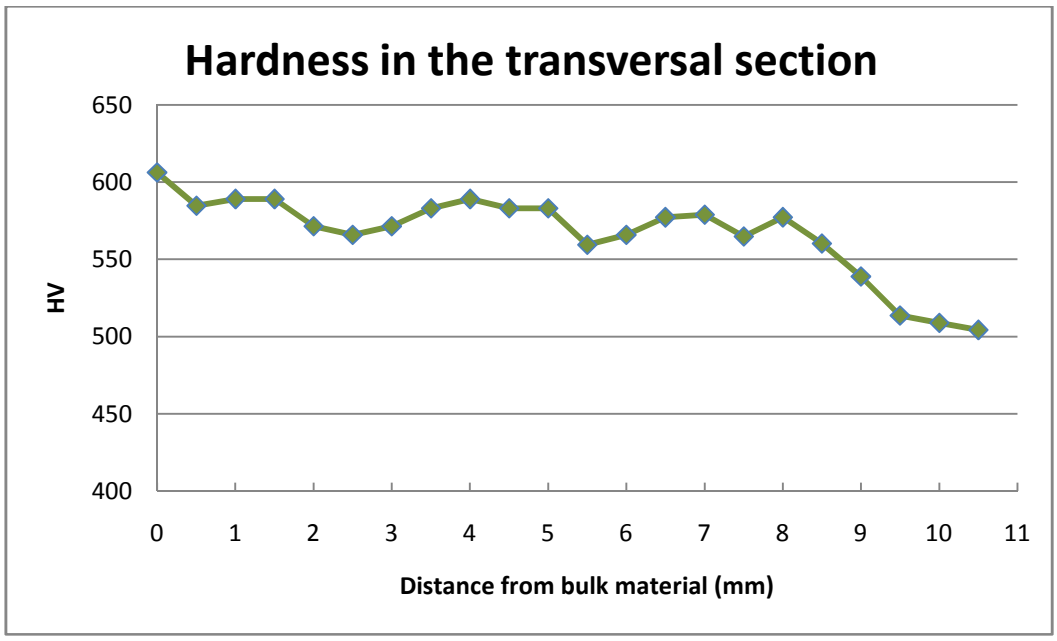

Figure 58. Hardness in the transversal section.

6.2.6 Residual stresses

From previous work by Kianzad (2015), a study of the residual stresses present in shot peened samples with an intensity of 0.4 mmA in one surface and 0.1 in the other was made. The following are the results from three samples. As expected, the compressive stresses are higher as the depth increases, until the depth is no longer influenced by the shot peened surface and the stresses tend to zero. The parameters of measure can be found in Appendix 4.

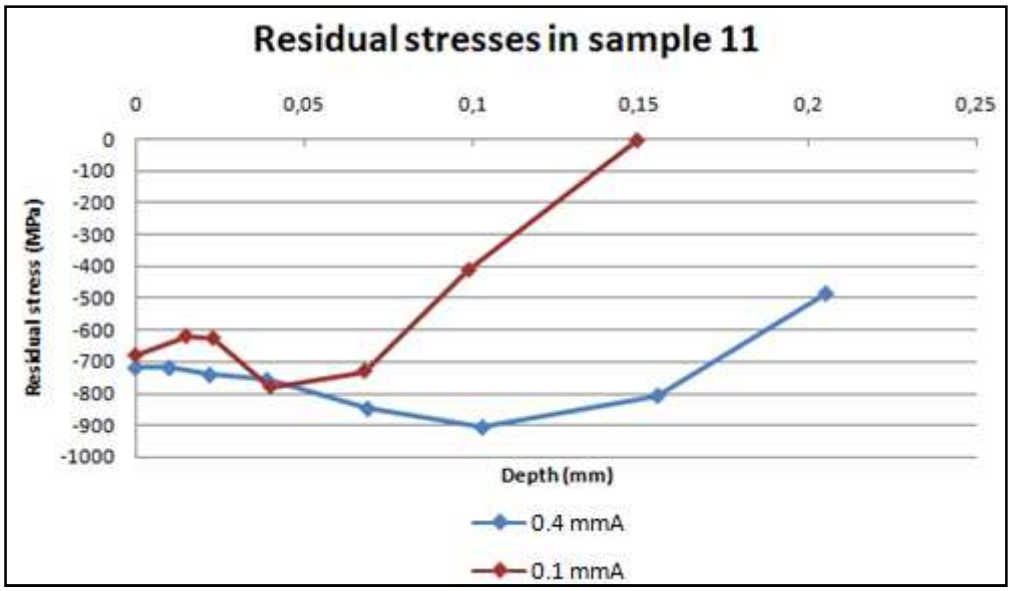

Figure 59. Residual stresses in sample 11.

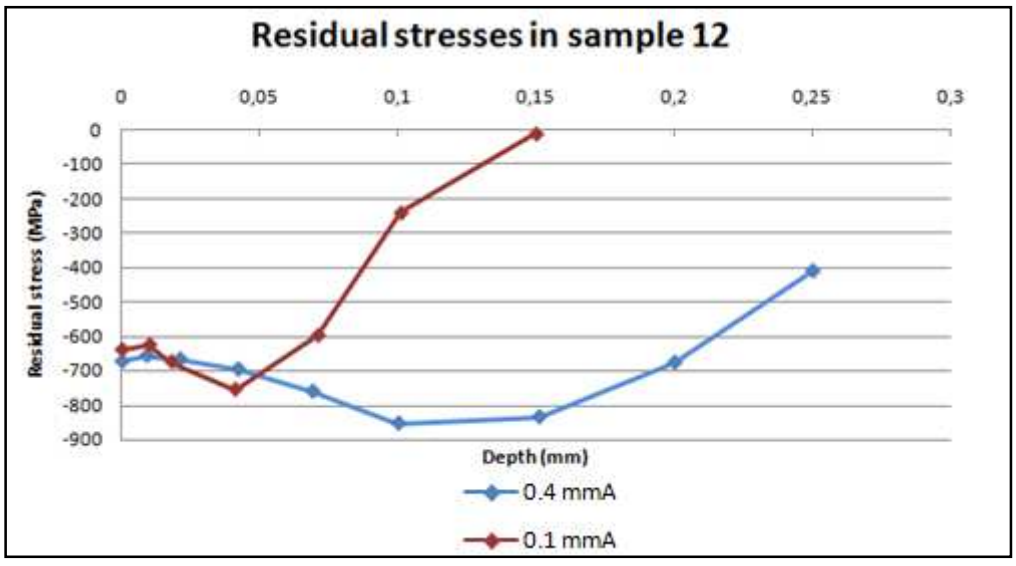

Figure 60. Residual stresses in sample 12.

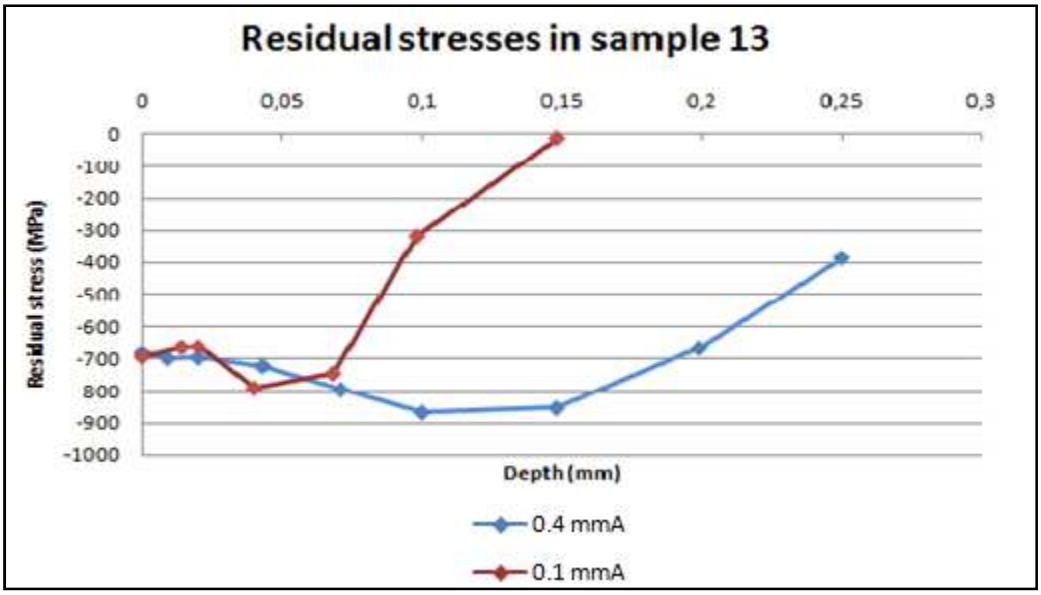

Figure 61. Residual stresses in sample 13.

7. DISCUSSION

After the study of the two surfaces shot peened at different intensities the main differences found were:

The root mean square parameter of roughness R_a was larger in the surface 1 with higher intensity, this surface has deeper hollows due to the higher energy and larger size of the shots. On the other hand surface 2 has more hollows but with less depth due to a lower energy and a larger amount of shots. Regarding the microstructure there is not much difference between the two surfaces but it can be observed that the shot peening layer is deeper in surface 1. The grain size is smaller near the surfaces which increases the mechanical properties such as strength and hardness and improves the fatigue life of the component and the fatigue crack resistance. It was confirmed that a higher intensity increases the hardness in the surface and in approximately 2 mm below the surface.

The results from the fatigue testing were not as successful as expected. It was confirmed that a lower intensity than 0.4 mmA increases the fatigue life. Although the samples that failed reached a low number of cycles, the endurance limit was higher with a lower intensity reaching 655 MPa which is far from the 990 MPa reached in previous work by Leiro (2014).

In the fracture analysis the microstructure bainite colonies with ferrite laths surrounded by films of retained austenite were observed. Defects were found all over the surface causing crack initiation and propagation. In the fracture surface initiation sites were found in the surface with no clear initiation of cracks. Inclusion was the cause of failure in one sample. In the transversal section of the fracture surface, the same defects and voids were found caused by continuous deformation during fatigue. These lead and provide an easier way for the cracks

to expand. It is clear that the crack occurs in the bainitic colonies and propagates trough the austenite films. In the X-ray diffraction test resulted on a lower content of retained austenite in the fracture surface. This fact is due to the TRIP-effect that takes place in fatigue testing in which austenite transforms into martensite during deformation. Also the results concluded that the content of retained austenite is higher as the applied stress increases which was the opposite of what was expected. As was expected the hardness decreases closer to the fracture surface.

8. CONCLUSIONS

In the fatigue test the endurance limit was lower than expected, however an increase in the fatigue life was observed compared with higher intensity shot peened samples from previous studies. The endurance limit was 655 MPa with a standard deviation of 86 MPa. A transformation of retained austenite into martensite in the fracture surface was observed in the X-Ray diffraction results due to the TRIP-effect caused during fatigue.

It was observed that the surface shot peened with a higher intensity had a larger damaged layer which can cause premature cracking in the surface during fatigue testing. The defects that were found are believed to improve crack propagation and initiation. One sample failed because of inclusion. It was observed that the initiation of cracks was placed in the surface.

The results of fatigue life in shot-peened samples were not as good as expected. Therefore after two studies both with a high and a low intensity it is possible that the hypothesis that shot-peening improves the fatigue life is not correct for this type of steel.

9. SUGESTIONS FOR FUTURE WORK

Studies have been made now of shot peened samples at intensities of 0.4 mmA and 0.1 mmA. For future work it would be useful to study the parameters of the shot peening in order to change them and improve the surface treatment reducing the surface damage which is where the initiation sites are and maintaining the compressive residual stressed layer.

Also it would be useful to make a more detailed study of the inclusions found to be graphite in order to study its carbon content and how this affects the crack initiation and propagation in the fatigue testing.

A study to compare the centre of not shot peened and shot peened samples would be helpful in order to study how this surface treatment affects in the transformation of austenite into martensite that takes place during deformation in fatigue testing.

10. REFERENCES

1. Honeycombe. R.W.K, Bhadeshia. H.K.D.H. (1995) *Steels, microstructure and properties.* Edward Arnold, London.
2. Callister. W.D, Rethwisch. D.G. (2007). *Materials science and engineering: An introduction.*Wiley, New york.
3. Bhadeshia. H.K.D.H. (1992) *Bainite in steels.* The institute of materials.
4. Sharma. S, Sangal. S, Mondal. K. (2011) *Development of New High-strength Carbide-Free bainitic steels.* Metallurgical and materials transactions A. Volume 42.
5. Totten. G.E. (2007).*Steel heat treatment handbook.* CRC Press
6. Leiro. A, Roshan. A, Sundin. K.G, Vuorinen. E, Prakash. B. (2013) *Fatigue of 0.55C-1.72Si Steel with tempered martensitic and carbide-free bainitic microstructures.* Acta Metallurgica Sinica.
7. Caballero. F.G, García-Mateo. C, Capdevilla. C, García de Andrés. C.(2007). *Advanced ultrahigh strength bainitic steels.* Materials and Manufacturing processes.
8. Leiro.A. (2014). *Microstructure analysis of wear and fatigue in high-Si austempered steels.* Luleå university of technology.
9. Caballero. F.G, Roelofs. H, Hasler. S, Capdevilla. C, Chao. J, Cornide. J, García-Mateo. C.(2012).*Influence of bainite morphology on impact toughness of continuously cooled cementite-free bainitic steels.* Materials, science and technology.
10. Wheelabrator shaping industry. http://www.wheelabratorgroup.com
11. Curtiss-wright. Metal improvement components. http://www.cwst.es/shot-peening-perdigoneado.html
12. Clark. A. (2013). *Comparison of austempering and quench-and-tempering processes for carburized automotive steels.* University of Windsor.
13. Belzunce Varela.F.J. Viña Olay.J.A. (2011). *Fundamentos de ciencia de los materiales*. E.P.S.de ingeniería de Gijón. Universidad de Oviedo.
14. Campbell. F.C. (2008). *Elements of metallurgy and engineering alloys.* ASM international.
15. Zahavi. E, Torbilo. V. (1996). *Fatigue design. Life expectancy of machine parts.* Boca Raton, CRC press.
16. Rice. R. C. (1997). *SAE fatigue design handbook.* Society of automotive engineers. Fatigue design and evaluation committee.
17. Schijve. J. (2001). *Fatigue of structures and materials.* Kluwer academic publishers. Dordrecht, Boston, London.
18. Rementeria. R, Morales-Rivas. L, Kuntz. M, Garcia-Mateo. C, Kerscher. E, Sourmail. T, Caballero. F.G. (2015). *On the role of microstructure in governing the fatigue behavior of nanostructured bainitic steels.* Materials science and engineering: A. Volume 630.
19. Wenyan. L, Jingxin. Q, Hesheng. S. (1997). *Fatigue crack growth behavior of a Si-Mn steel with carbide-free lathy bainite.* Journal of materials science. Volume 32.
20. Yokoi. T, Kawasaki. K, Takahashi. M, Koyama. K, Mizui. M. (1996) *Fatigue properties of high strength steels containing retained austenite.* JSAE Review. Volume 17.

21. Throop. J. F, Reemsnyder. H. S. (1982). *Residual stress effects in fatigue.* ASTM special technical publication 776.

22. De los Rios. E. R, Walley. A, Milan. M. T, Hammersley. G. (1995). *Fatigue crack initiation and propagation on shot-peened surfaces in A316 stainless steel.* International Journal of Fatigue. Volume 17.

23. Tekeli. S. (2002). *Enhancement of fatigue strength of SAE 9245 steel by shot-peening.* Materials letters. Volume 57.

24. Dalaei. K, Karlsson. B, Svensson. L. E. (2011). *Stability of shot peening induced residual stresses and influence on fatigue lifetime.* Materials science and engineering, A.

25. Vielma. A. T, Llaneza. V, Belzunce. F. J. (2014). *Effect of coverage and double peening treatments on the fatigue life of a quenched and tempered structural steel.* Surface and coatings technology. Volume 249.

26. Meguid. S. A. (1986). *Impact surface treatment.* Elsevier applied science publishers.

27. Little. R. E, Ekvall. J.C. (1981). *Statistical analysis of fatigue data.* American society for testing and materials.

28. Kianzad. S. (2015). *Fatigue properties of shot-peened Carbide-free bainitic steels.* Luleå university of technology

29. Begouin. C, Dardevet. M, Garcia. O, Hell. J. (2016). *Shot blasting of steel.* Surface engineering project. Luleå university of technology.

APPENDIX

1. Microstructure

Pictures from SEM of the cross section of the shot peened sample with different intensities.

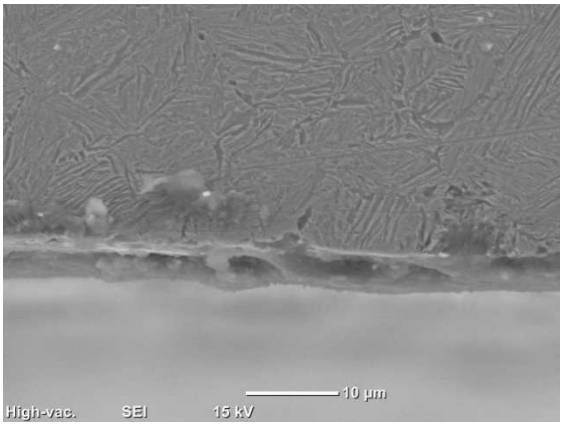

Figure 1. Surface 1 in SEM

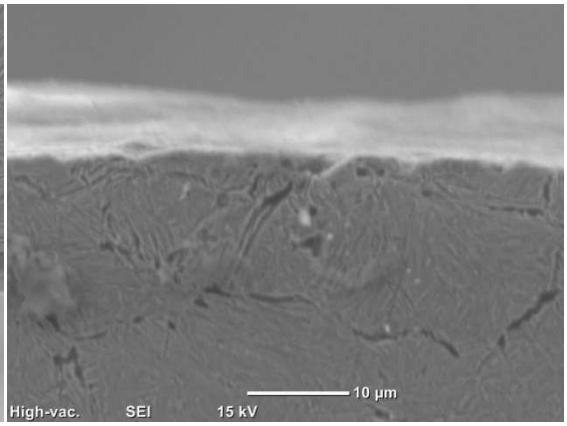

Figure 2. Surface 2 in SEM

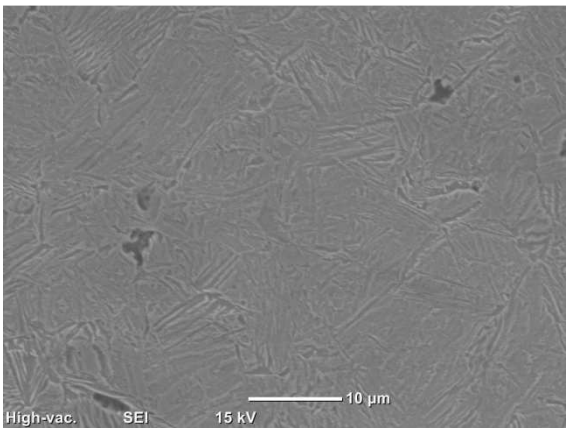

Figure 3. Bulk material in SEM

2. Hardness

Table 1. Measures of the surface 1 and 2 hardness

	Surface 1	Surface 2
1	651,5	632,4
2	684,4	652,7
3	719	599,9
4	703	652
5	612	686,3
6	703	703,9
7	673,4	652,9
8	665,4	688,5
9	665	685,9
10	638,1	666,6
11	625	658,4
12	688,5	625,8
13	687,7	645,2
14	680,7	679,7
15	695,7	673,3
Mean	672,8	660,2

3. Fracture analysis

Pictures of the failure surface:

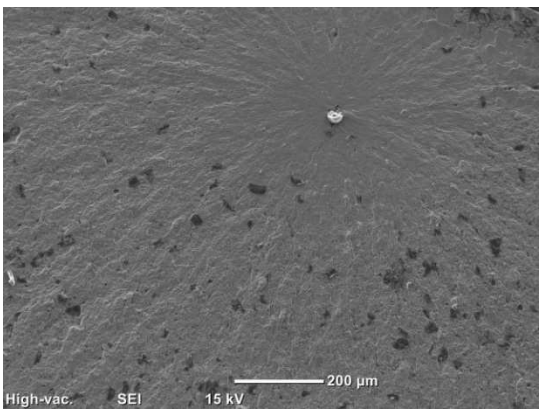

Figure 4. Inclusion

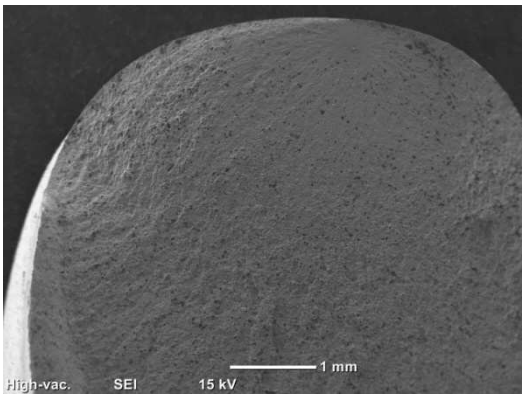

Figure 5. Fracture surface

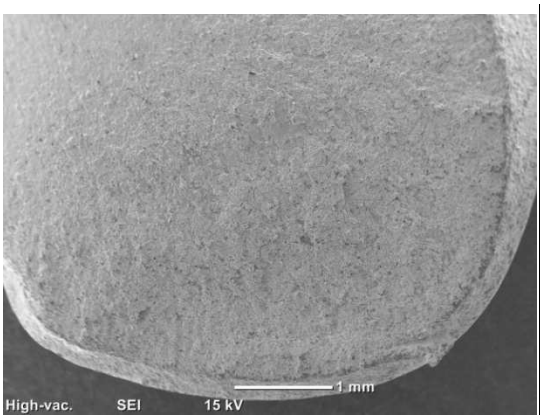

Figure 6. Fracture surface.

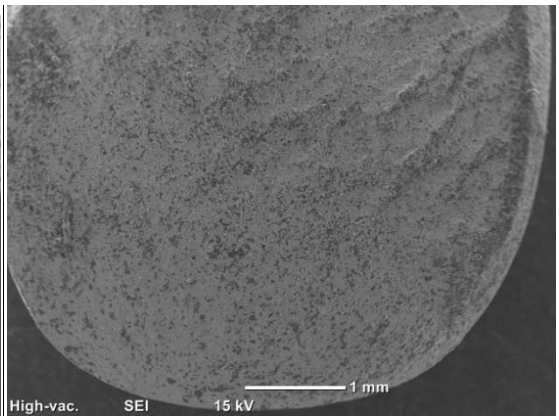

Figure 7. Fracture surface.

Pictures of the transversal section of the fracture surface:

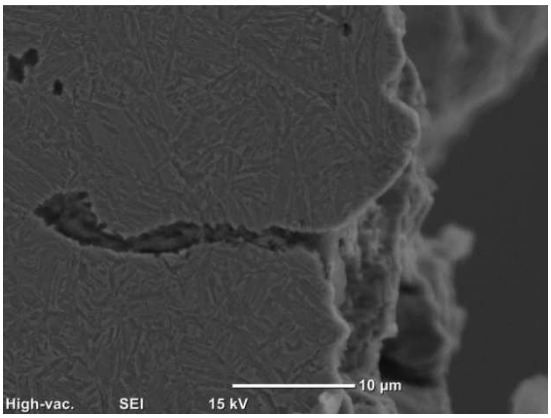

Figure 8. Crack propagation.

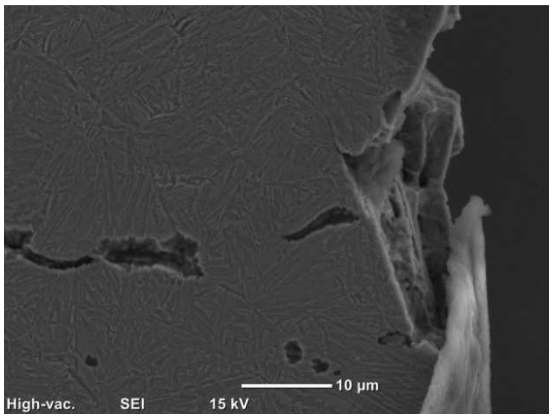

Figure 9. Crack initiation.

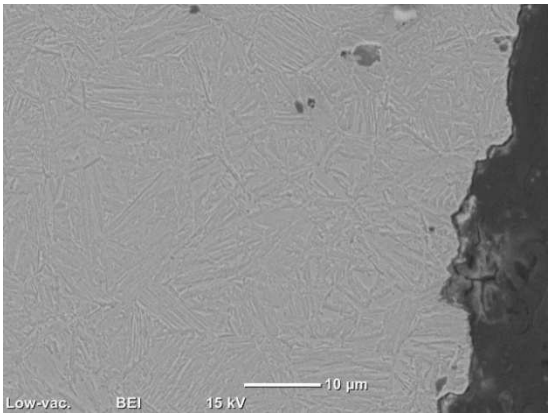

Figure 11. T-S of fracture surface.

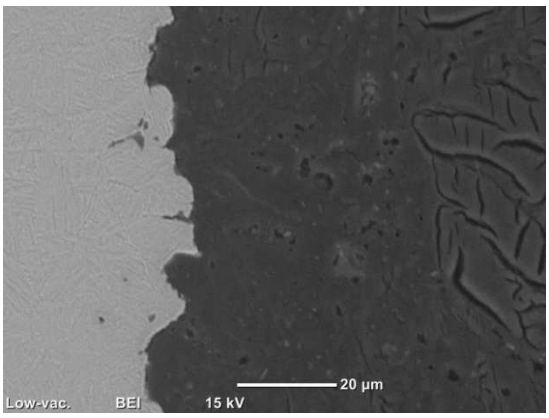

Figure 12. T-S of fracture surface.

4. Residual stresses

Parameters of measure:

Stress Calculation		Corrections	
φ offset	0	Peak limits	Disabled
Calc. shear stresses	Disabled	Smoothing	Disabled
Calc. princ. stresses	Enabled	Bg sub.	Enabled
Princ. stresses method	Regression from all rotations	Bg type	Constant
Calc. stress tensor	Disabled	Bg pixels	30
Peak Position		Kα 2 corr.	Disabled
Peak shift	Cross correlation	Material Data	
Parab. lvl	85	Poiss. ratio	0.3
Threshold	20	Young's mod	211000
2θ pos.	Calibrated	Set Expr.	Disabled
Det. used	A and B	2θ val.	156.4
		Used K	Using Kα

5. Inclusion analysis

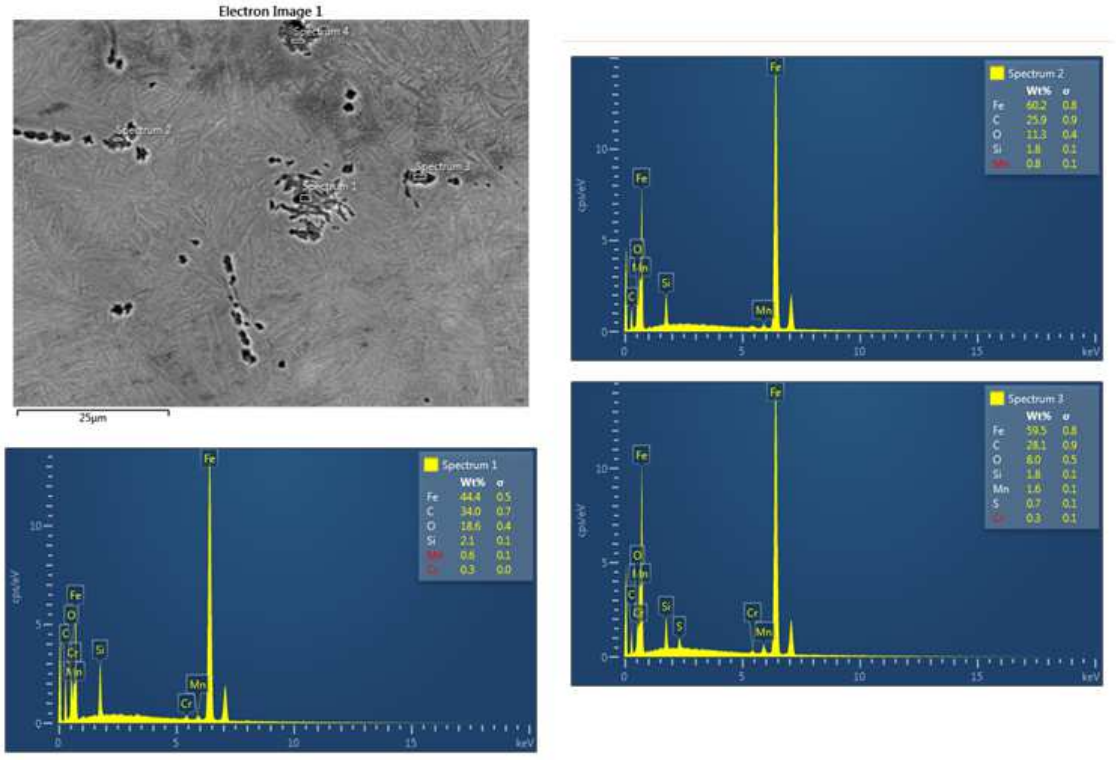

Figure 13. Inclusion analysis in SEM